SCHOOL on Generation IV reactors fuel cycle

Thermodynamic aspects of nuclear fuels (Modelling)

Christine Guéneau
Den-Service de Corrosion et du Comportement des Matériaux dans leur Environnement
CEA, Université Paris-Saclay
91191 Gif-sur-Yvette, France

13-17 May 2019, Delft, The Netherlands

Outline

1 - The Calphad method

2 - Basic Gibbs energy models

3 - Modelling of the U-Pu-O system

- 3.1 U-O
- 3.2 Pu-O
- 3.3 U-Pu-O

4 - Calculations on a irradiated MOX fuel

5 - Conclusion

The Gibbs energy

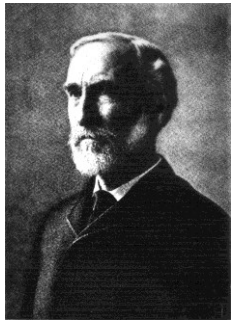

Josiah Willard Gibbs (1839-1903)

- The Gibbs energy of a system is defined by:

$$G = H - TS = U + PV - TS$$

- H is the enthalpy ⇨ heat content of the system
- T is the temperature
- S is the entropy of the system ⇨ randomness of the system
- U is the internal energy of the system ⇨ kinetic and potential energies of atoms
- P is the pressure
- V is the volume

vibrations — bonds

- G is the **key function** in thermodynamics of materials
- At constant temperature and pressure, a closed system (fixed mass and composition) will be in stable equilibrium if it has the lowest value of the Gibbs energy:

$$dG = 0$$

Thermodynamic equilibrium

- $G = H - TS$

⇨Compromise between low enthalpy and high entropy

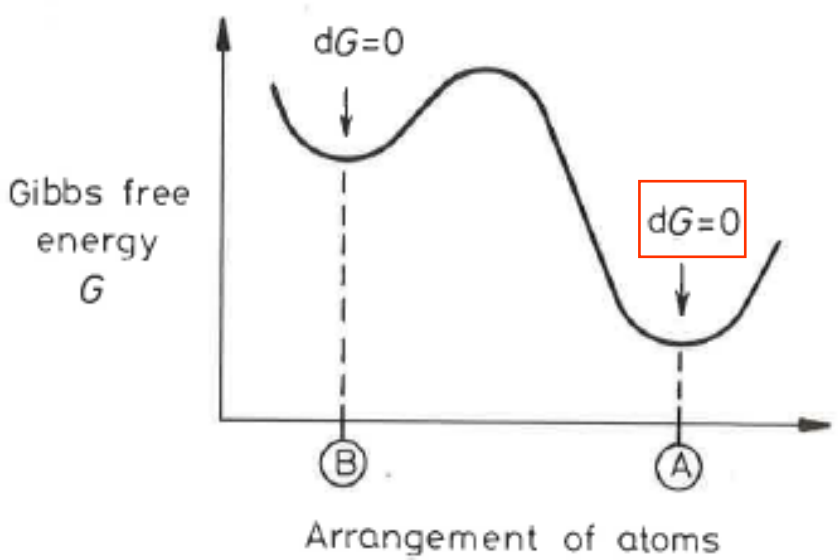

⇨The A configuration is the lowest possible value of G ⇨ Equilibrium

⇨The B configuration is a metastable equilibrium state (local equilibrium)

⇨The intermediate configurations are unstable

⇨The rate at which the system will reach the equilibrium is not provided by thermodynamics

The Gibbs energy

⇨ Thermodynamic potential at given P, T, n

$$G = U + PV - TS = H - TS$$

- $H = U + PV$ ➡ Enthalpy (U: internal energy)
- $\left(\frac{\partial G}{\partial T}\right)_{P,N_i} = -S$ ➡ Entropy
- $\left(\frac{\partial G}{\partial N_i}\right)_{T,P,N_{j\neq i}} = \mu_i$ ➡ Chemical potential
- $C_P = -T\left(\frac{\partial^2 G}{\partial T^2}\right)_{P,N_i}$ ➡ Heat capacity

⇨ Key thermodynamic properties to describe the phases

Gibbs energy minimization

- At given T, P, n_i the equilibrium corresponds to the minimum of the Gibbs energy of the system:

$$dG = 0$$

- The Gibbs energy of the system G is a linear combination of the Gibbs energies of the phases, G_m^{φ} :

$$G = \sum_i m^{\varphi} G_m^{\varphi}$$

m^{φ}: mole fraction of phase φ

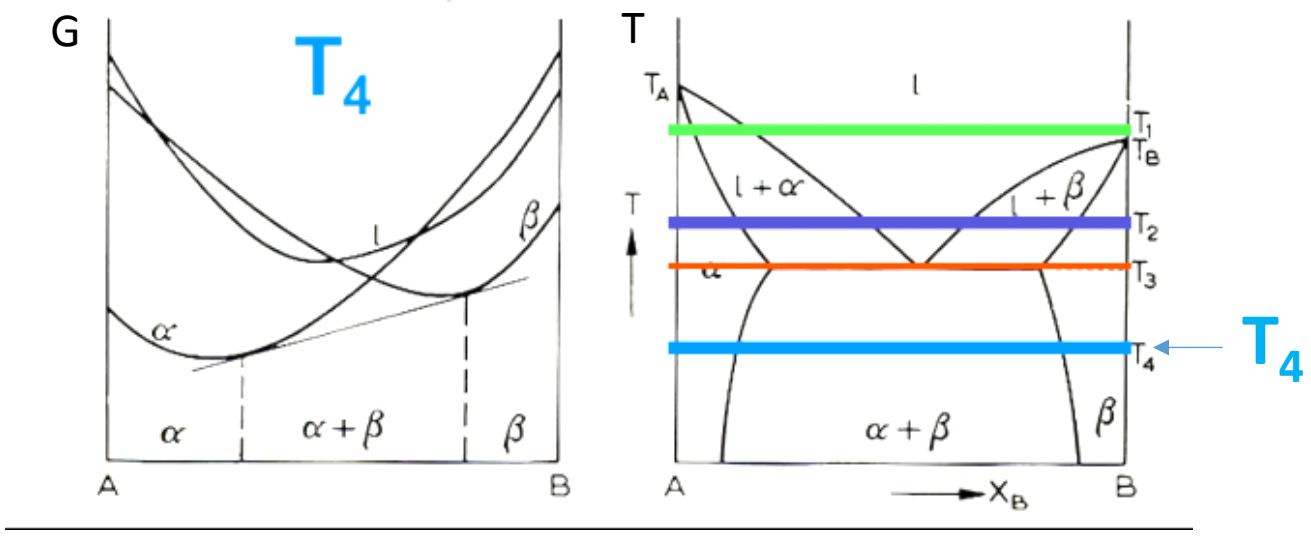

CALPHAD (CALculation of PHAse Diagram) method:

- At given T, P, n_i the equilibrium is calculated by minimization of the Gibbs energy of the system: $dG = 0$

⇨ Coupling Gibbs energies and phase diagrams

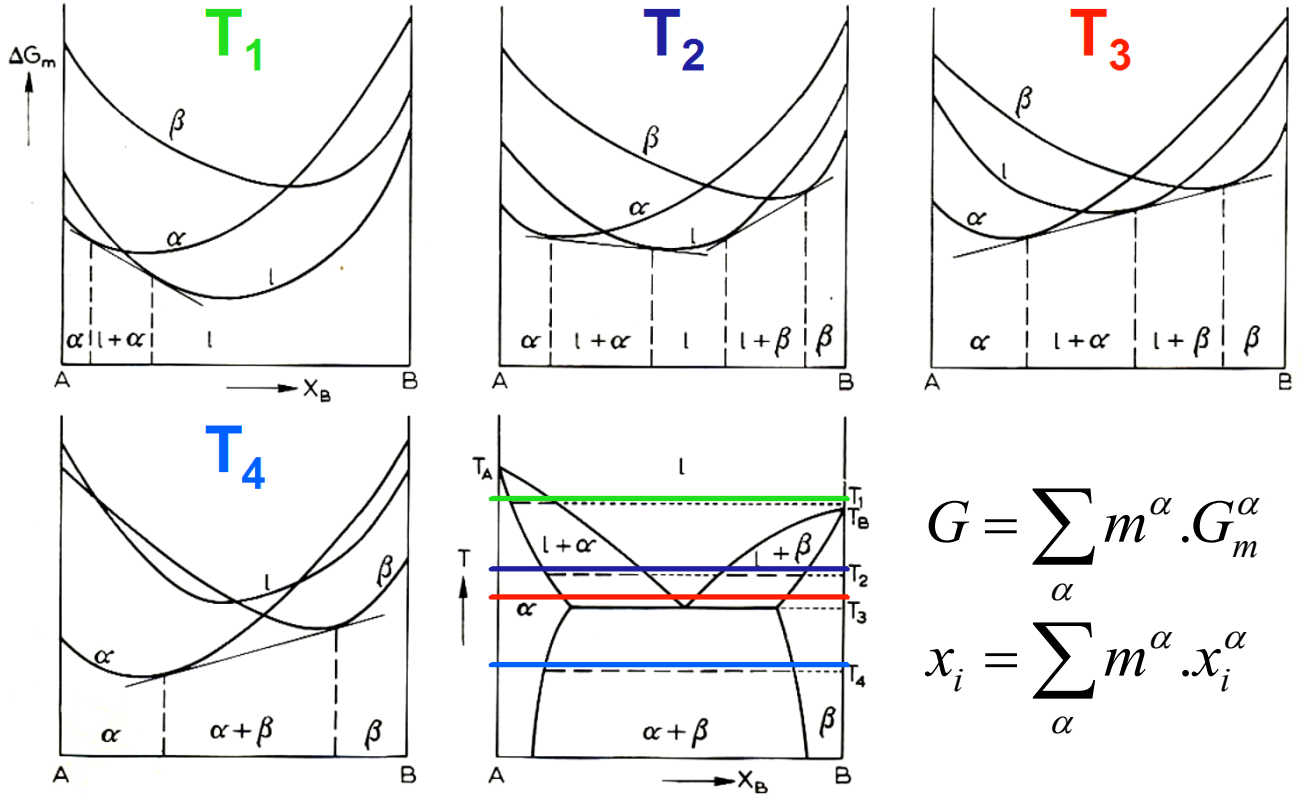

$$G = \sum_{\alpha} m^{\alpha} . G_m^{\alpha}$$

$$x_i = \sum_{\alpha} m^{\alpha} . x_i^{\alpha}$$

$$\min(G) = \min\left(\sum_{\alpha} m^{\alpha} G_m^{\alpha}(T, p, x_i^{\alpha} \text{ or } y_k^{(l,\alpha)}) \right)$$

The phase diagram can be calculated from the phases Gibbs energies

Calphad modeling

➡ Assessment procedure

- Mathematical functions are chosen to describe the Gibbs energy of the phases

$$G_m^{\alpha}(T, p, x_i^{\alpha} or\ y_k^{(l,\alpha)})$$

- The variables are assessed by a least-square minimizing method to reproduce the available thermodynamic and phase diagram data

- For a multi-component system, the equilibrium is calculated by extrapolation from models for binary and ternary sub-systems

➡ Good prediction of both phase diagram and phase thermodynamic data for multi-component systems

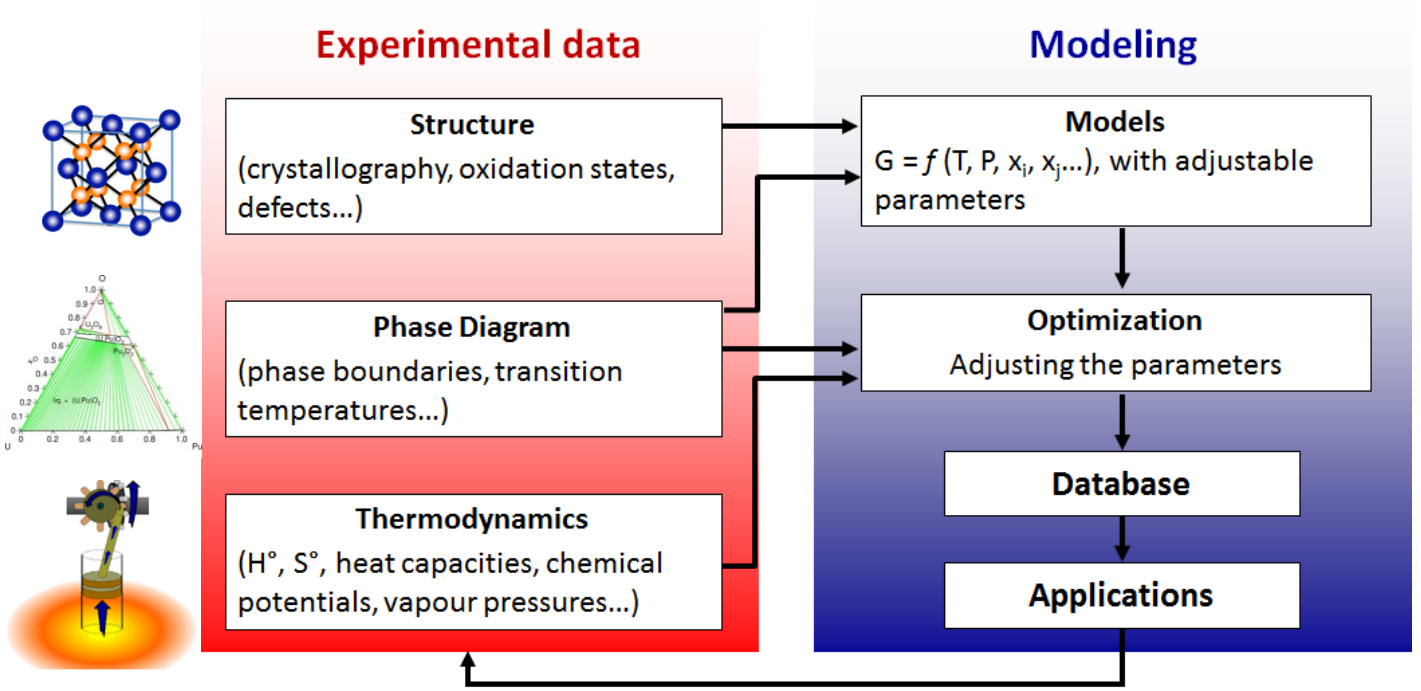

➡ SATA (School on Advanced Thermodynamic Assessment)

➡ Sublattice model to describe the phases

- Connection between thermodynamics and crystallography ➡ **Sublattice modeling**
- **The sublattices correspond to equivalent positions** i.e. sites belonging to the same Wyckoff position
- To simplify the model, several sets of equivalent positions may be combined and treated as a single sublattice

➡ A single sublattice model is used for all the phases with the same crystalline structure

FCC (Faced centered cubic)

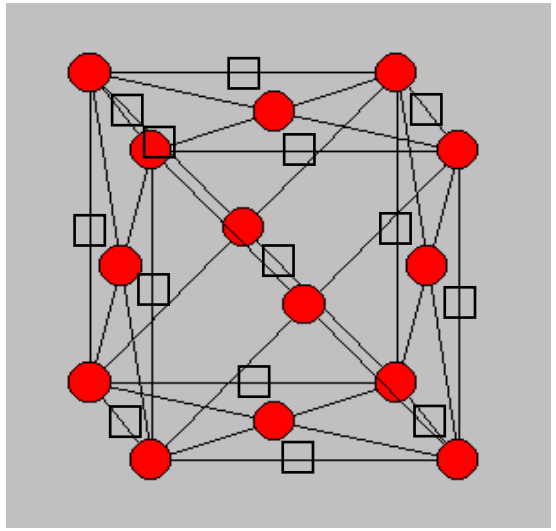

(A)1(Va)1

● Atom A
□ Vacant site (Va)

BCC (Body centered cubic)

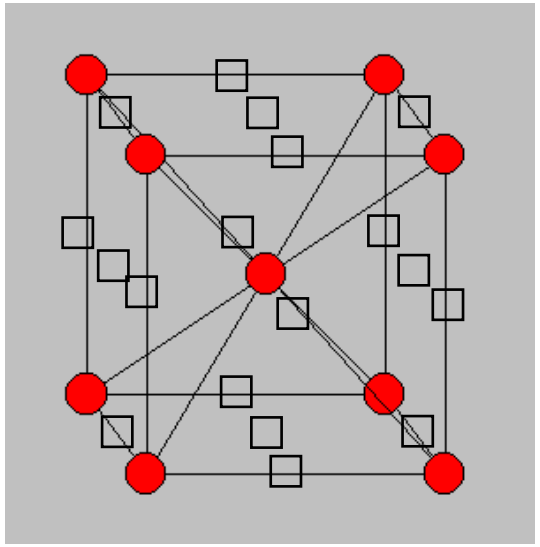

(A)1(Va)3

Sublattice 1: Substitutional site for metals A, B, C ….
Sublattice 2: Interstitial site for O, C, N …

Model for phases with a fixed composition

⇨ Pure elements, stoichiometric compounds

- G_m^α is **the molar Gibbs energy of the phase α,** refered to the enthalpy of the pure elements in their stable state at 298.15 K and 1 bar (**SER: Stable Element Reference**).

$$\Rightarrow G_m^\alpha - \sum_i b_i H_i^{SER} = a_0 + a_1 T + a_2 T lnT + a_3 T^2 + a_4 T^{-1} + a_5 T^3 \ldots$$

b_i is the stoichiometric coefficient of the element i in the phase α

$$H = G + T\,S = G - T\left(\frac{\partial G}{\partial T}\right)_{p,N_i}, \quad S = -\left(\frac{\partial G}{\partial T}\right)_{p,N_i}, \quad C_p = -T\left(\frac{\partial^2 G}{\partial T^2}\right)_{p,N_i}$$

$$H_m^\alpha - \sum_i b_i H_i^{SER} = a_0 - a_2 T - a_3 T^2 + 2a_4 T^{-1} - 3a_5 T^3 + \ldots$$

$$S_m^\alpha = -a_1 - a_2(1 + lnT) - 2a_3 T + a_4 T^{-2} - 3a_5 T^2 + \ldots$$

$$C_p^\alpha = -a_2 - 2a_3 T - 2a_4 T^{-2} - 6a_5 T^2 + \ldots$$

Model for a regular solution (A,B)

Influence of the interaction parameter L_{AB} on the phase diagram

$$G_m^{\alpha} = x_A \, {}^{\circ}G_A + x_B \, {}^{\circ}G_B + RT(x_A ln x_A + x_B ln x_B) + x_A x_B \, L_{AB}$$

G reference — G ideal — G excess

L < 0

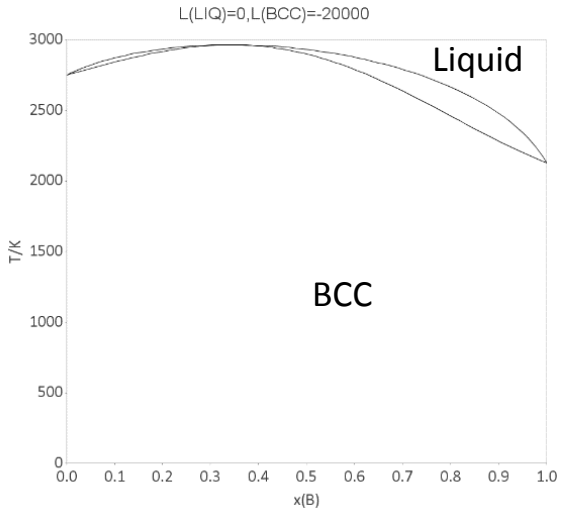

L = 0

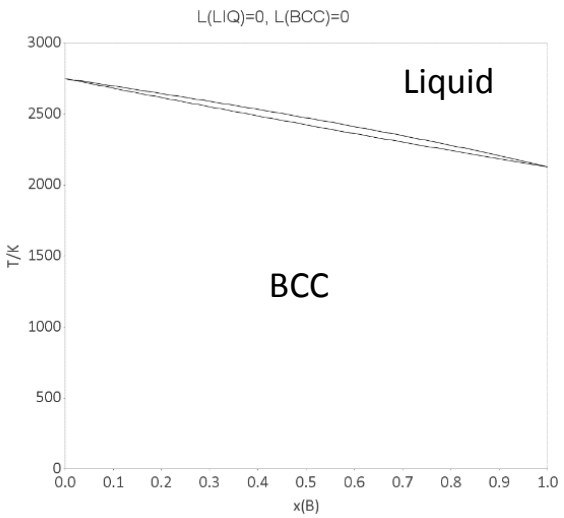

L > 0

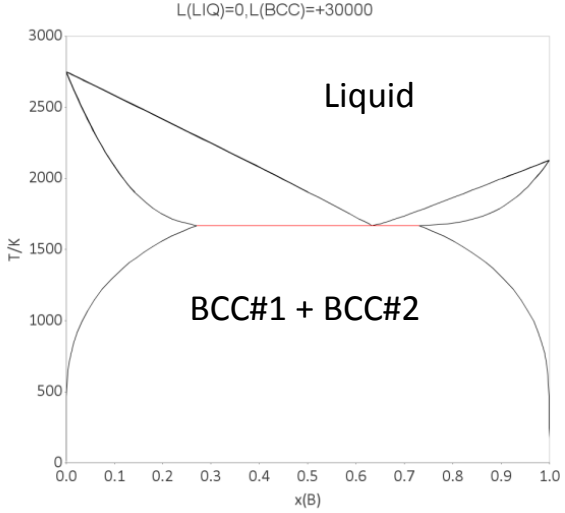

L(BCC) = -20000
Stabilization

L(BCC) = 0
Ideal solution

L(BCC) = +30000
Phase separation
(Miscibility gap)

Model for a real solution (A,B)

Dependence in composition of the interaction parameter ➡ **Redlich-Kister**

$$G_m^{\alpha} = x_A \, {}^{\circ}G_A + x_B \, {}^{\circ}G_B + RT(x_A ln x_A + x_B ln x_B) + x_A x_B \, L_{AB}$$

$$\Rightarrow L_{AB} = \sum_{v=0} (x_A - x_B)^v \, v_{L_{AB}} = {}^0L_{AB} + {}^1L_{AB}\,(x_A - x_B) + {}^2L_{AB}\,(x_A - x_B)^2 + ..$$

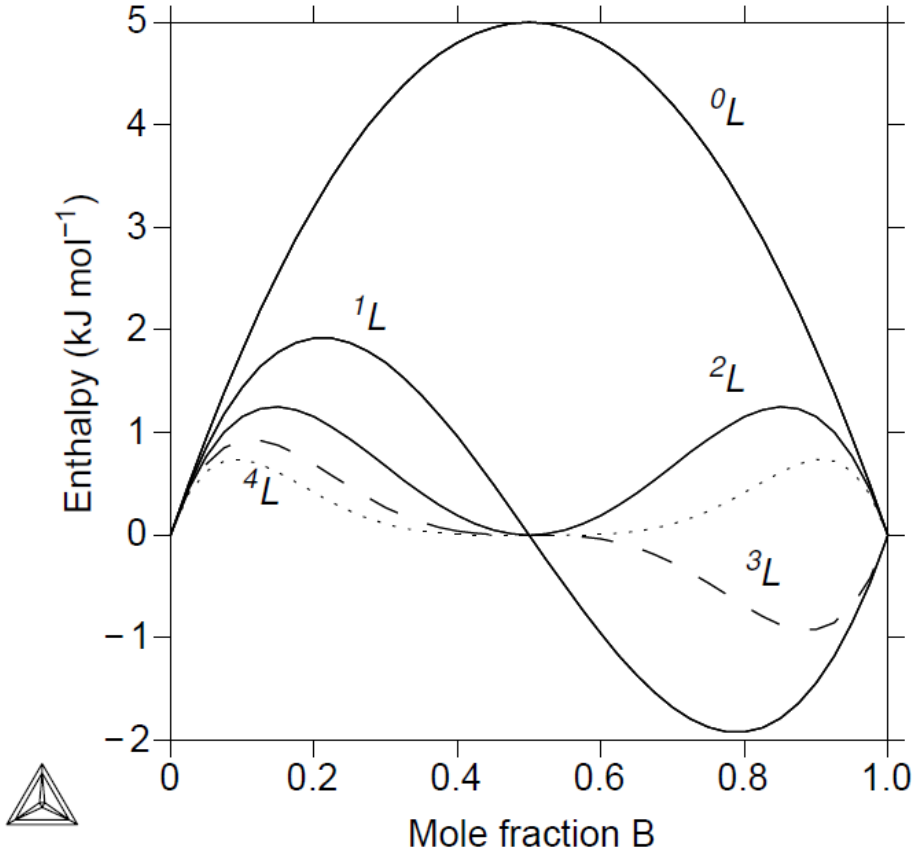

$${}^vL_{AB} = 20000$$

How to model the U-Pu-O system ?

1st step: modeling of the U-O, Pu-O and U-Pu binary sub-systems

- Binary interaction parameters for solutions
- G functions for the binary compounds

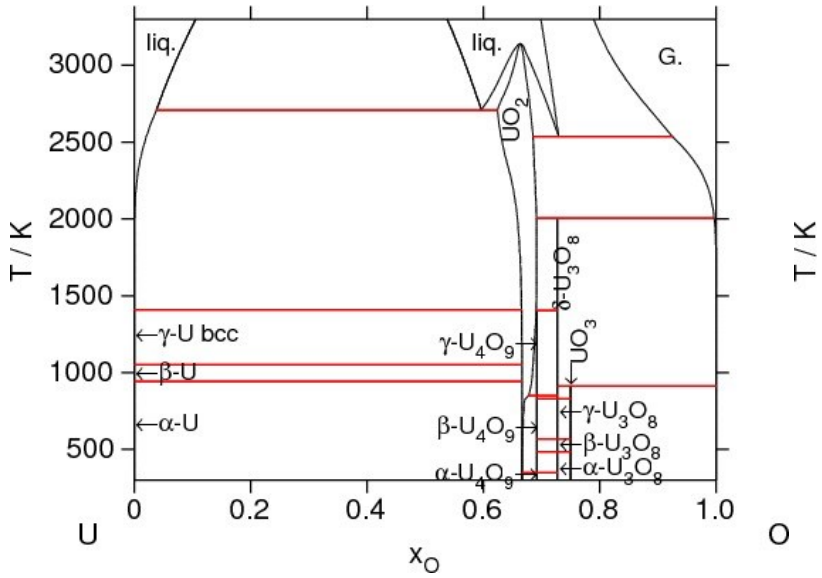

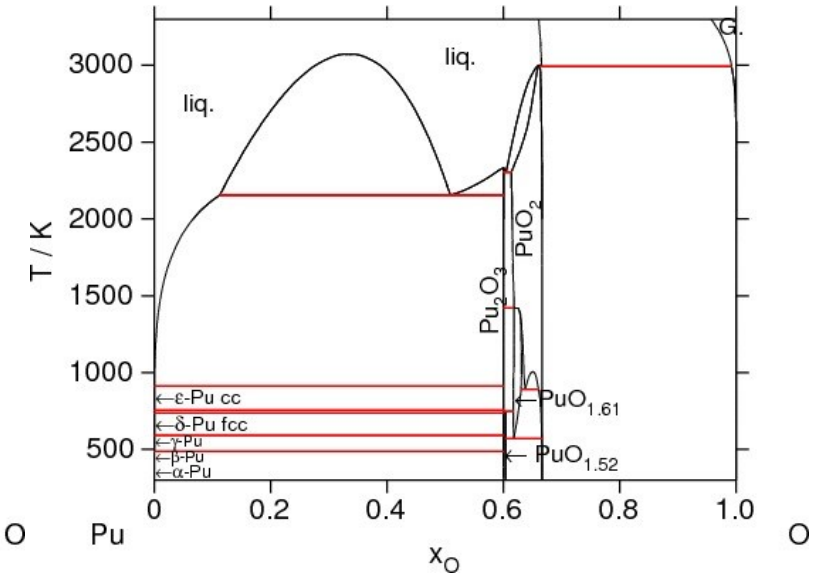

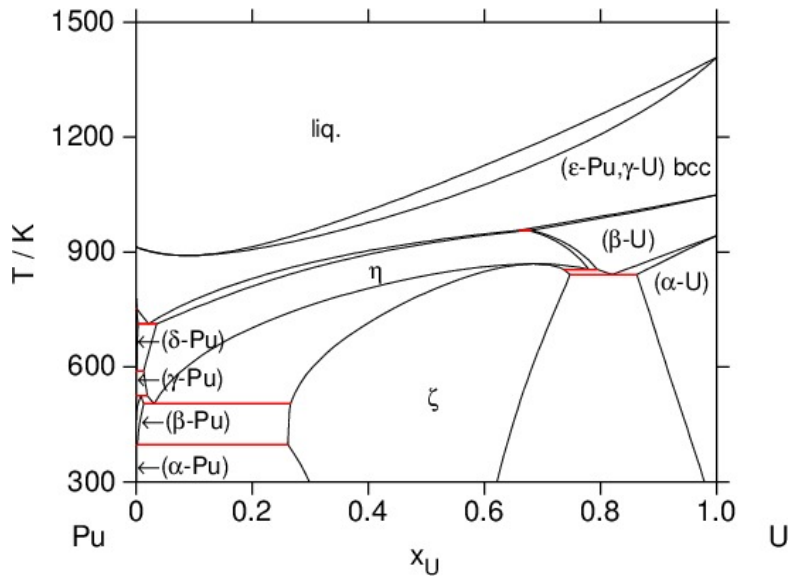

2nd step: modeling of the U-Pu-O ternary system

- Ternary interaction parameters for solutions
- G functions for the ternary compounds

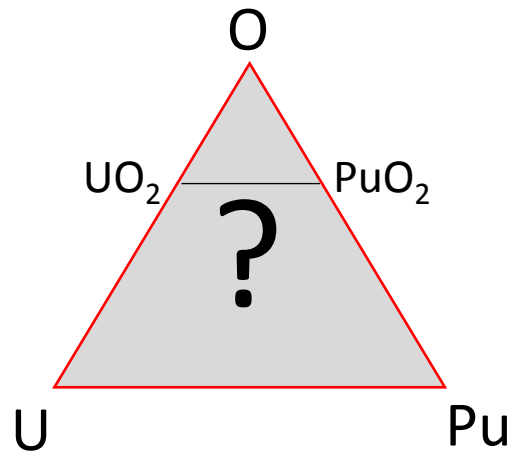

➡ Sublattice model for non stoichiometric $UO_{2\pm x}$

■ Uranium dioxide $UO_{2\pm x}$ with fluorite structure has a large oxygen composition range

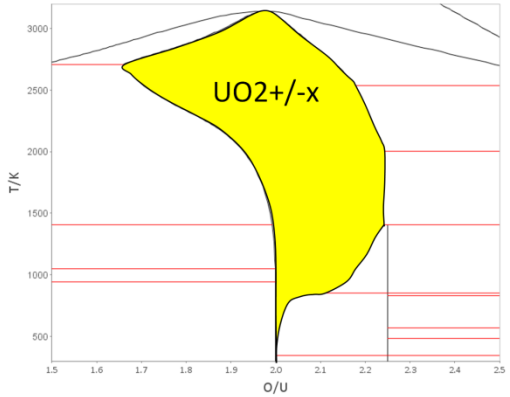

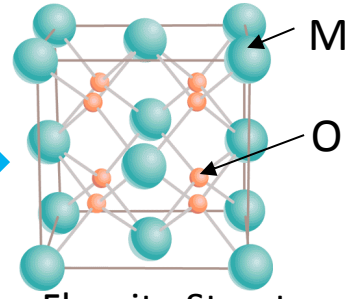

Fluorite Structure

■Compound Energy Formalism + Three sublattice model $(U^{+3},U^{+4},U^{+5})\ (O^{-2},Va)_2\ (O^{-2},Va)$

➡Formation of oxygen vacancies and interstitials compensated by reduction/oxidation of U^{+4} into U^{+3}/U^{+5}

12 end-members

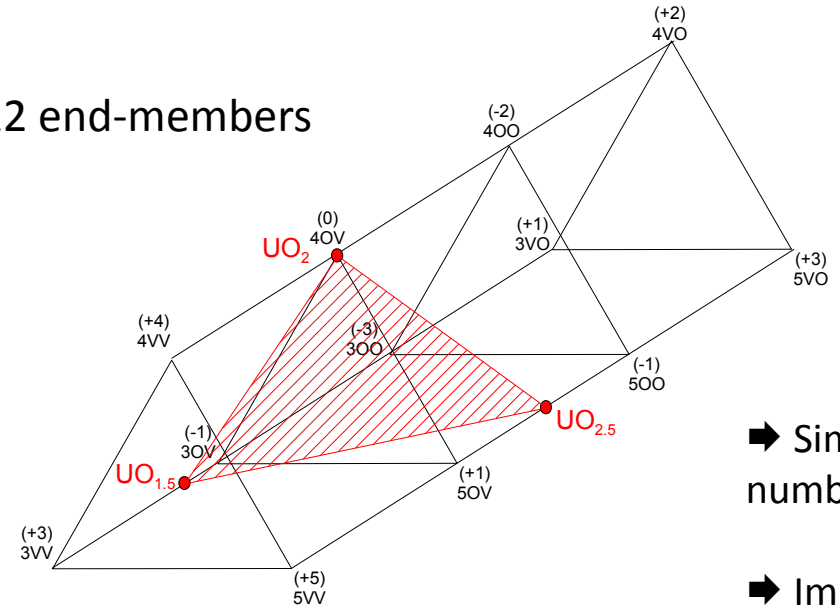

[Guéneau et al, JNM 419 (2011) 145]

$$
\begin{aligned}
G_m^{UO_2} = {} & y_3 y_O y'_V\, G^0_{3OV} + y_3 y_V y'_V\, G^0_{3VV} + y_3 y_O y'_O\, G^0_{3OO} + y_3 y_V y'_O\, G^0_{3VO} \\
& + y_4 y_O y'_V\, G^0_{4OV} + y_4 y_V y'_V\, G^0_{4VV} + y_4 y_O y'_O\, G^0_{4OO} + y_4 y_V y'_O\, G^0_{4VO} \\
& + y_5 y_O y'_V\, G^0_{5OV} + y_5 y_V y'_V\, G^0_{5VV} + y_5 y_O y'_O\, G^0_{5OO} + y_5 y_V y'_O\, G^0_{5VO} \\
& + RT\left(y_3 \ln y_3 + y_4 \ln y_4 + y_5 \ln y_5\right) \\
& + 2RT\left(y_O \ln y_O + y_V \ln y_V\right) + RT\left(y'_O \ln y'_O + y'_V \ln y'_V\right) \\
& + G_m^{Excess}
\end{aligned}
$$

➡ Simple relationships between G parameters for the end-members are fixed to decrease the number of variables to be optimized

➡ Important parameters are: $G(UO_{1.5})$, $G(UO_2)$, $G(UO_{2.5})$

➡ Thermodynamic properties for stoichiometric UO_2

- Even in stoichiometric UO_2, point defects (Oxygen Frenkel pairs, electronic defects) form at high temperature

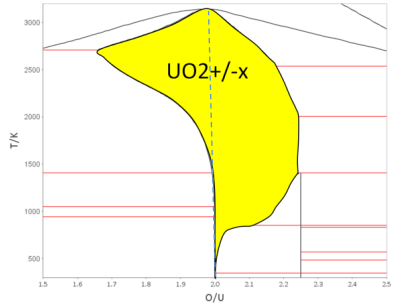

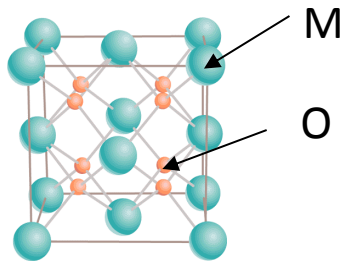

Fluorite Structure

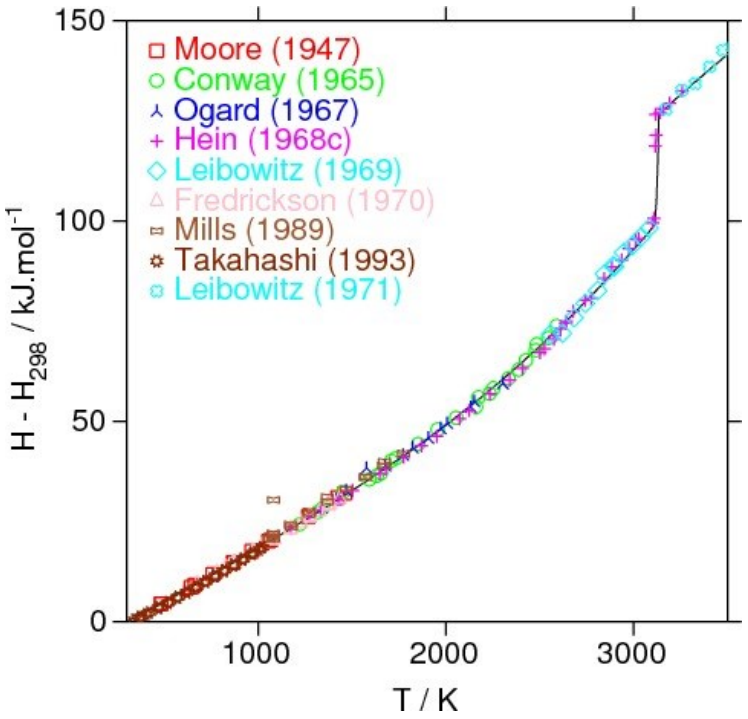

$$C_P = \left(\frac{\partial H}{\partial T}\right)_{P,N_i}$$

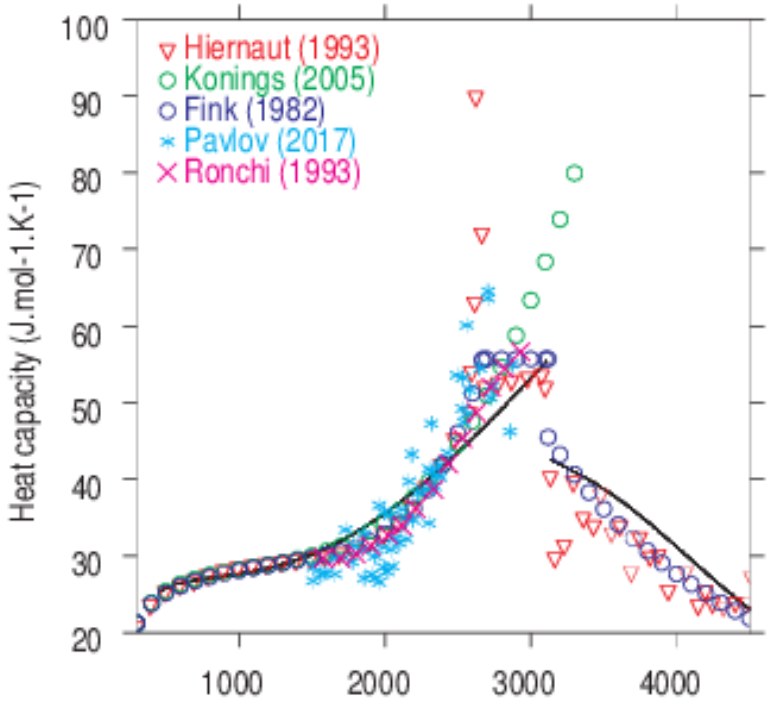

➡ The increase in the heat capacity for T>1500 K is due to the increase in point defect concentration

[Guéneau et al, JNM 419 (2011) 145]

[Pavlov et al, Acta Materialia 139 (2017) 138]

➡ Thermodynamic data on non stoichiometric $UO_{2\pm x}$

- Experimental oxygen and uranium chemical potential data are available

$$\mu_{O_2} = \overline{\Delta G}(O_2) = R\,T \ln p_{O_2}$$

$$\mu_U = \overline{\Delta G}(U) = R\,T \ln a_U$$

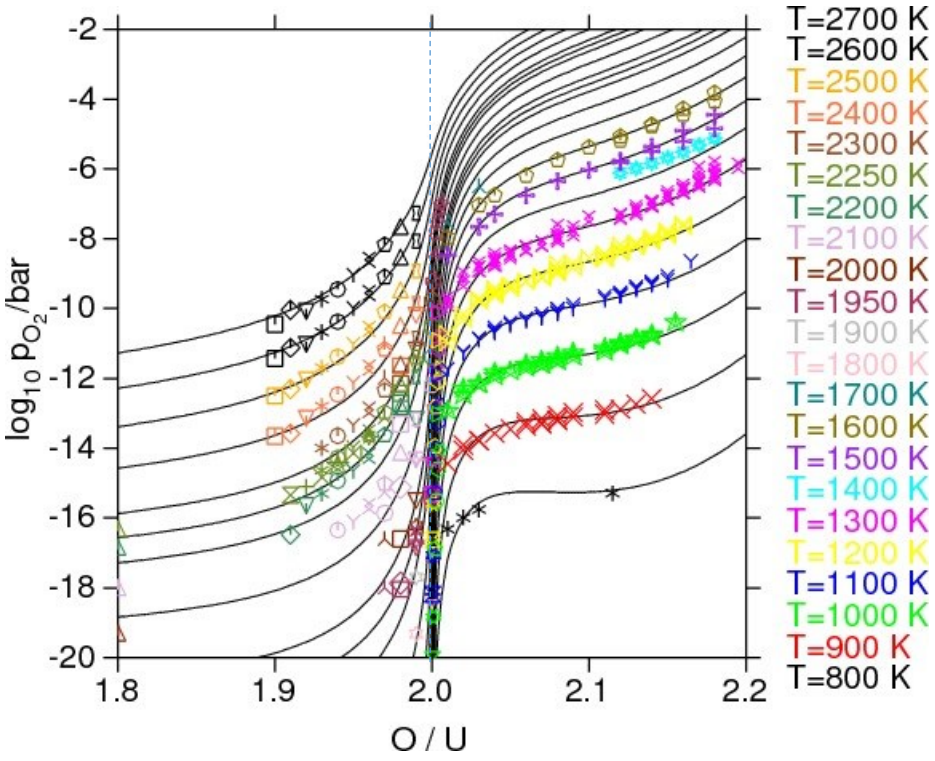

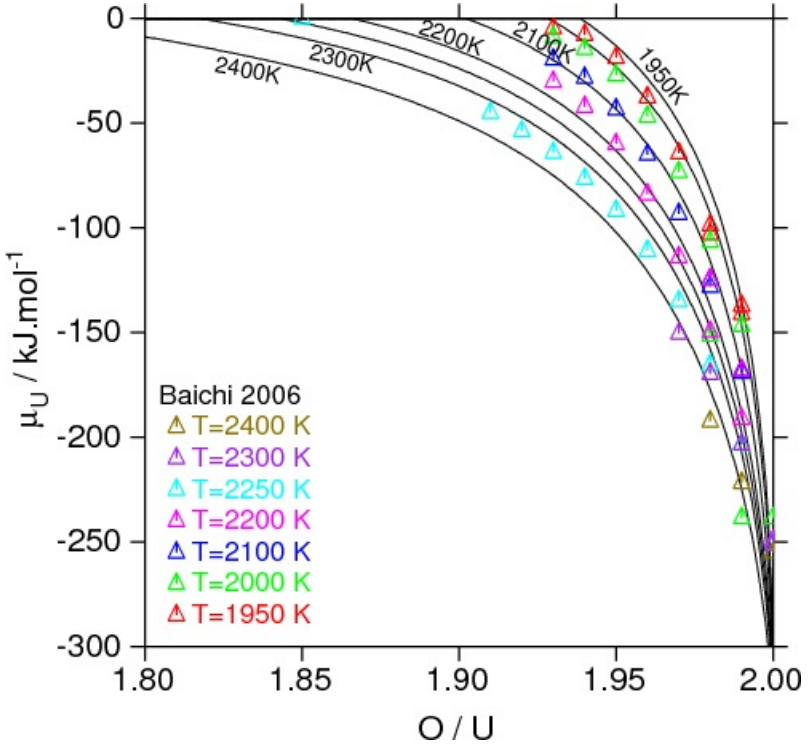

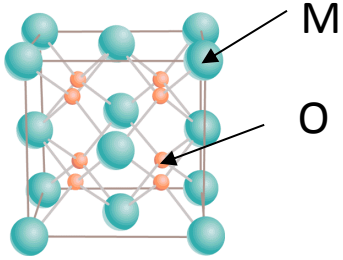

Fluorite Structure

➡ The oxygen and uranium chemical potentials vary strongly with oxygen stoichiometry

[Guéneau et al, JNM 419 (2011) 145]

➡ Thermodynamic data on non stoichiometric $UO_{2\pm x}$

- The oxygen potential variation is related to point defect concentration:
  - O/M<2: $(U^{+3},U^{+4})\ (O^{-2},Va)_2\ (Va)$ ⇨ Oxygen vacancies and U^{+3}
  - O/M>2: $(U^{+4},U^{+5})\ (O^{-2})_2\ (O^{-2},Va)$ ⇨ Oxygen interstitials and U^{+5}

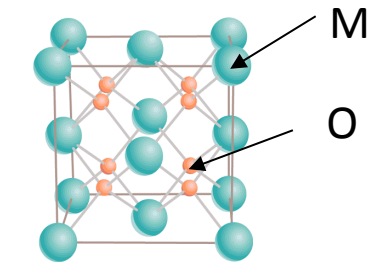

Fluorite Structure

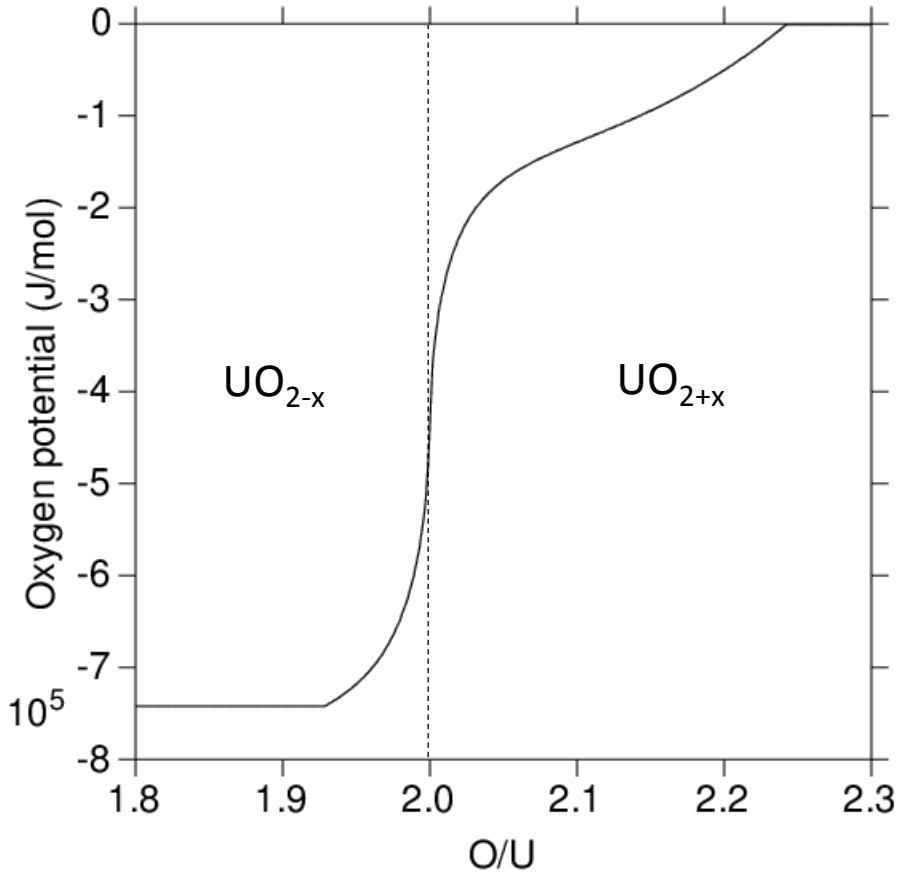

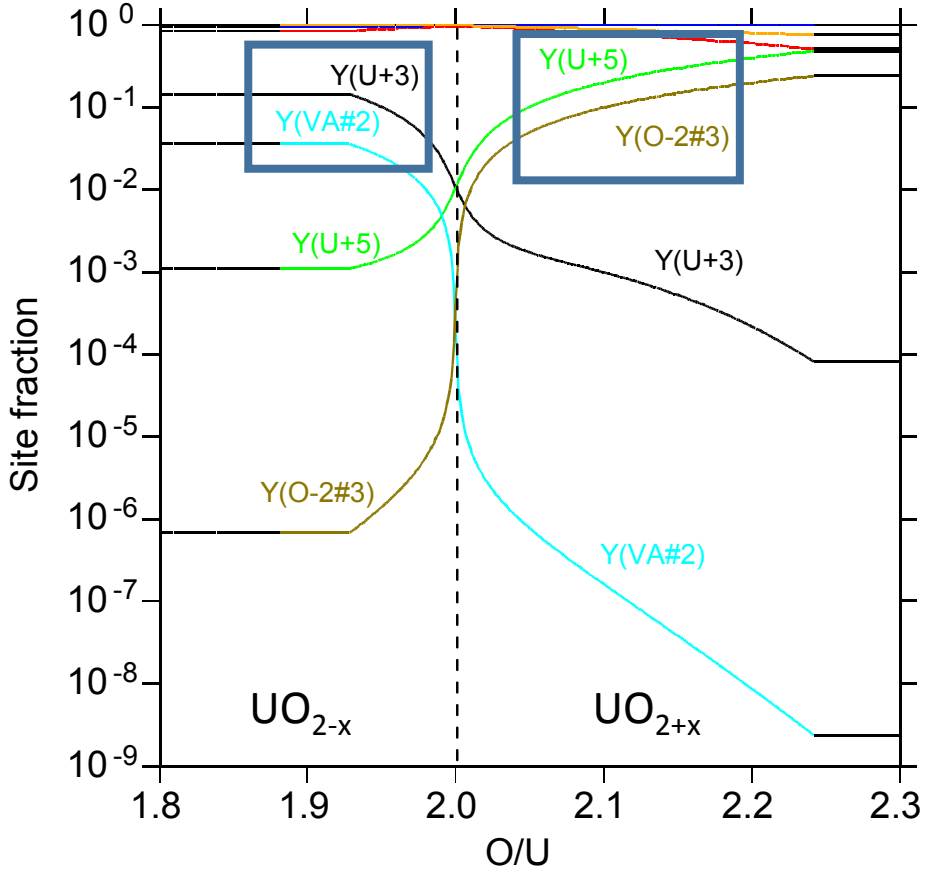

[Guéneau et al, JNM 419 (2011) 145]

➡Phase diagram data on the U-O system

Phase diagram data

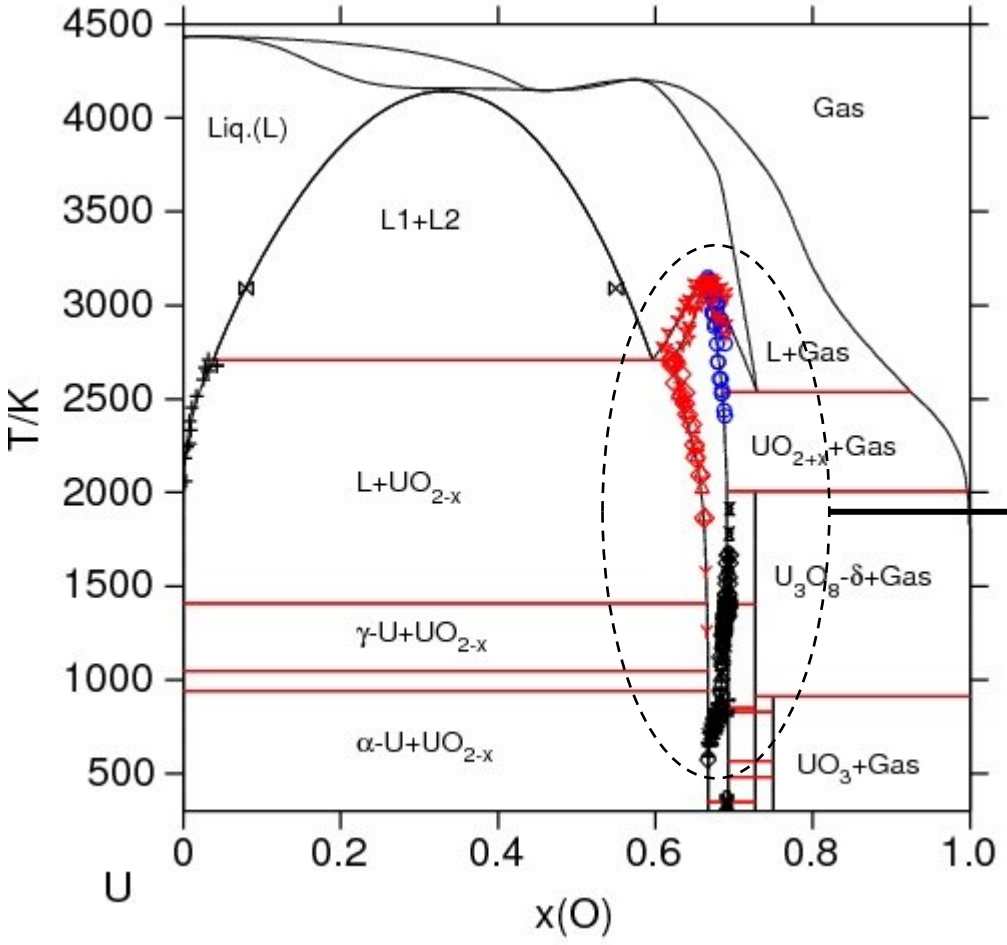

[Guéneau et al, JNM 419 (2011) 145]

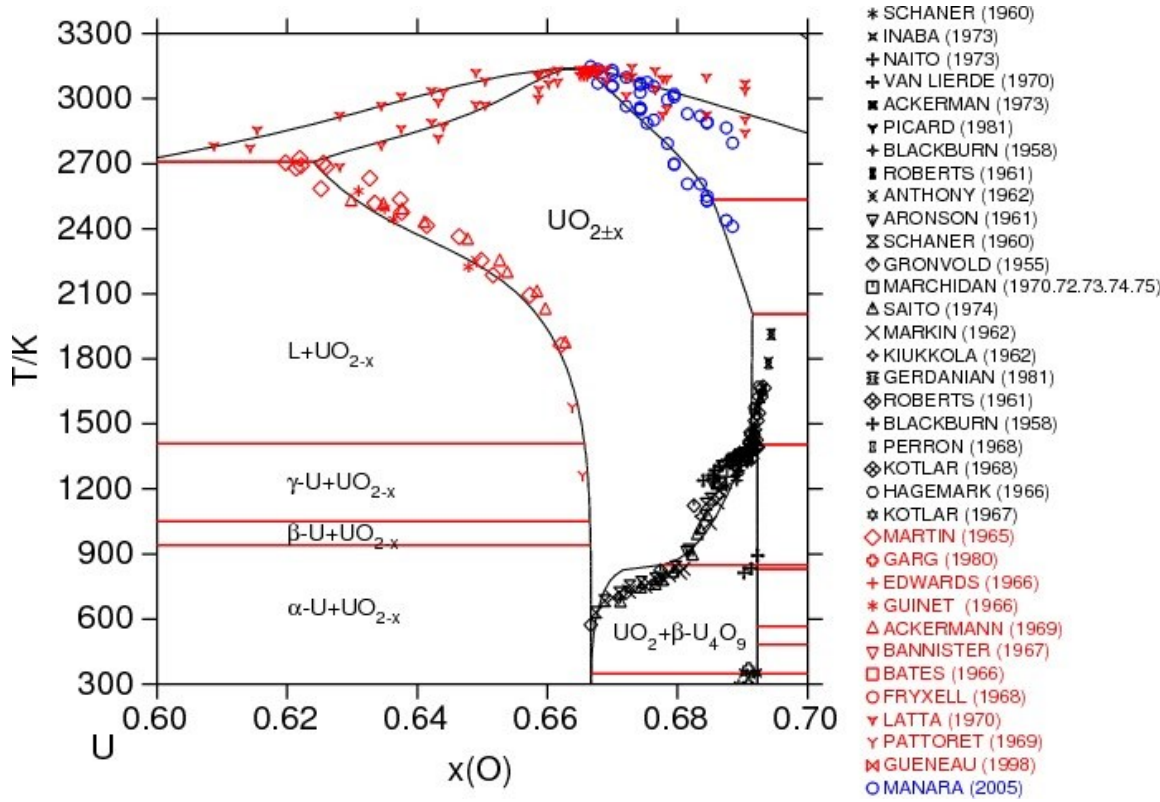

○ D. Manara – Laser heating
T solidus/liquidus for UO_{2+x}

[Manara et al, JNM 362 (2007) 14]

➡ Thermodynamic data on non stoichiometric PuO_{2-x}

- Plutonium dioxide PuO_{2-x} has a large oxygen composition range with O/Pu<2

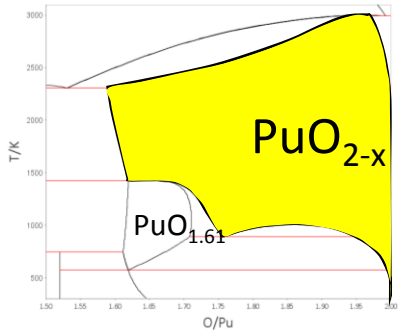

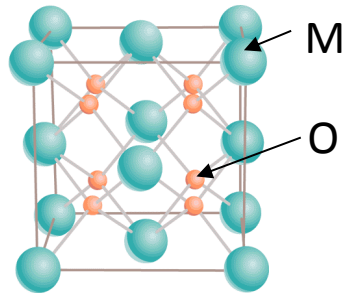

Fluorite Structure

- **Three sublattice model $(Pu^{+3},Pu^{+4})\ (O^{-2},Va)_2\ (Va)$**

➡ **Formation of oxygen vacancies (Va) compensated by reduction of Pu^{+4} into Pu^{+3}**

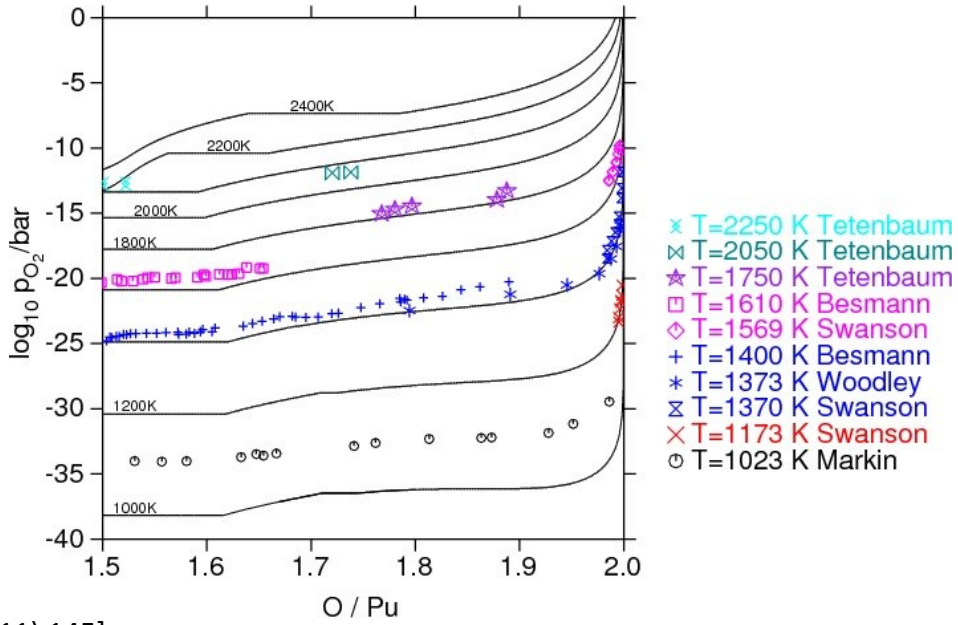

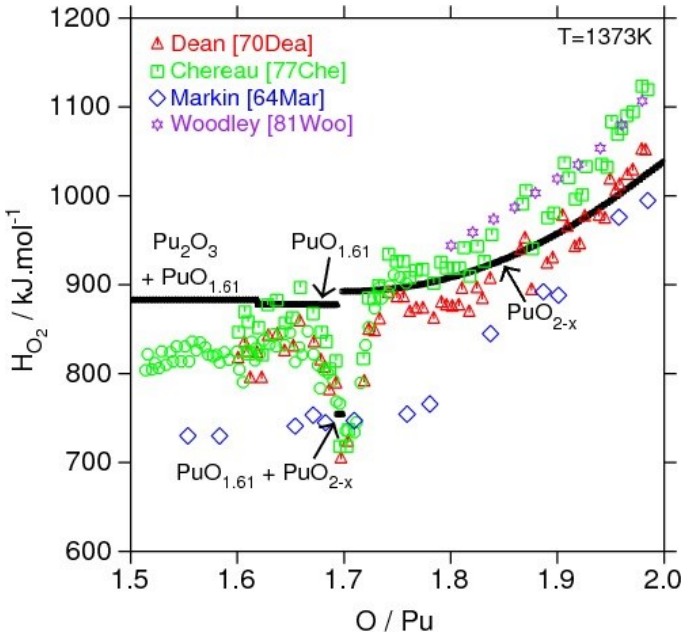

[Guéneau et al, JNM 419 (2011) 145]

➡ Phase diagram data on the Pu-O system

Phase diagram

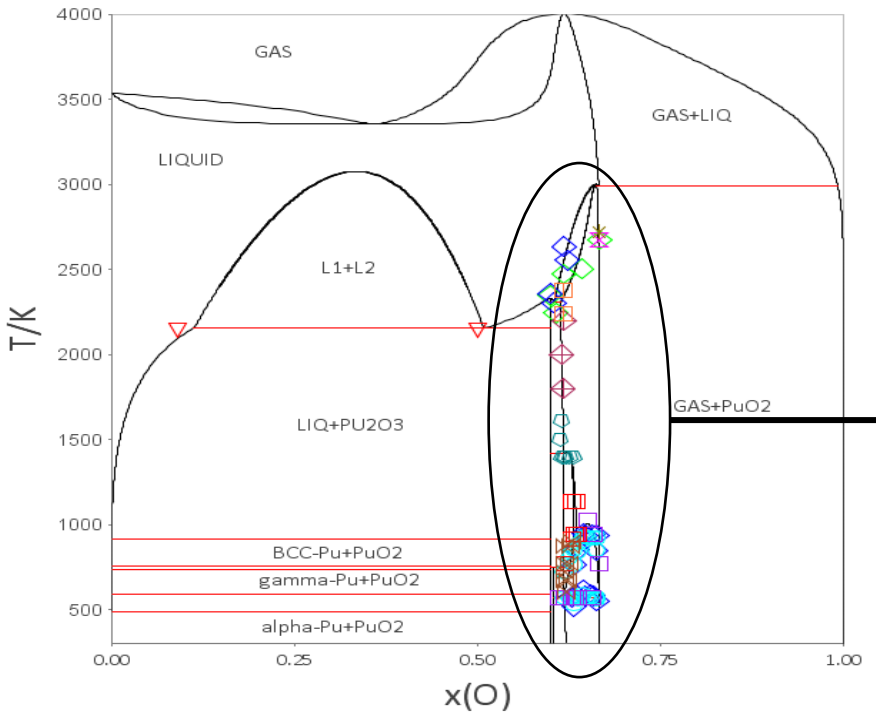

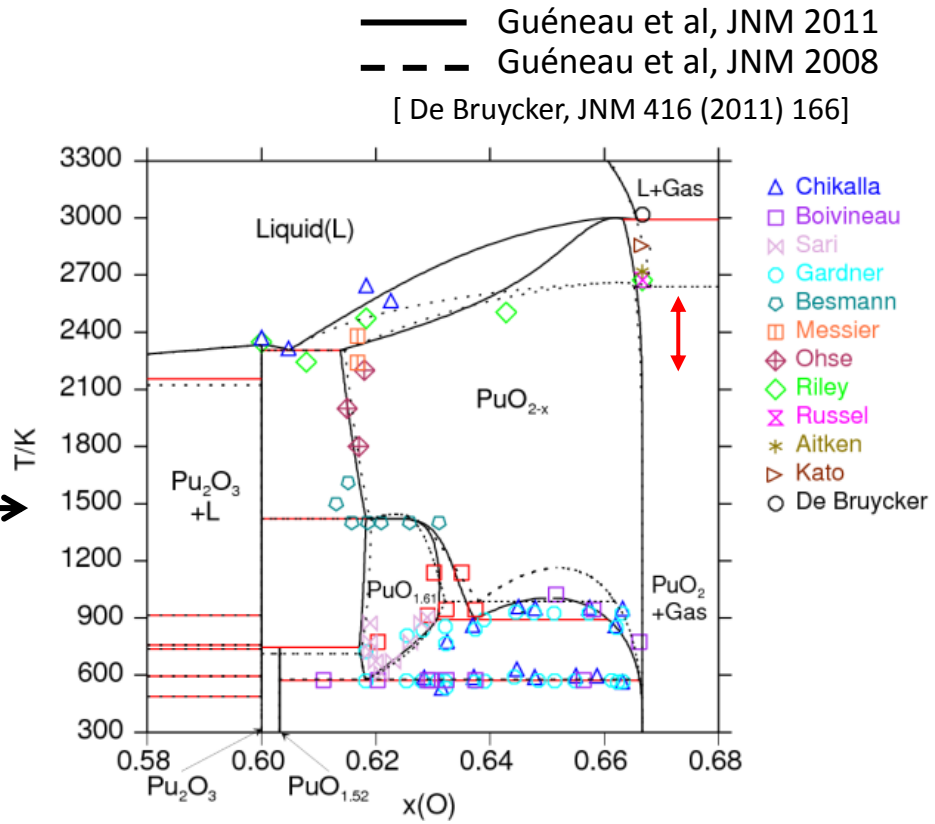

The experimental data on melting point data of PuO_2 are very scattered:

- The « **reference** » data (**2670-2700 K**) from the 60's-70's measured by thermal analysis in **W crucible**
- In 2005, Kato et al performed measurements (**2850 K**) using thermal analysis and **Re crucible**
- In 2010, De Bruycker et al did new measurements (**3017 K**) using **laser heating (self-crucible)**

➡ΔT ~ 300 K between old and recent measurements !!

➡ According to the calculations, PuO_2 loses oxygen below its melting point ➡ Congruent melting for O/Pu<2

[Guéneau et al, JNM 419 (2011) 145]

➡Melting point data on actinide oxides

Why such large discrepancies bewteen old and new measurements ?

$\mu(O_2)=\overline{\Delta G}(O_2)=RT\ln(p(O_2))$

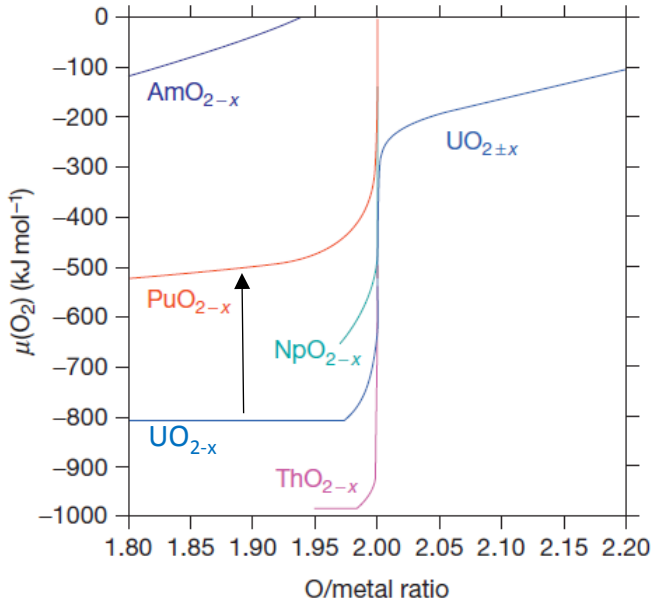

[Guéneau et al, Chap. 2.02, Comp. Nuc. Mater. (2012)]

Melting point data

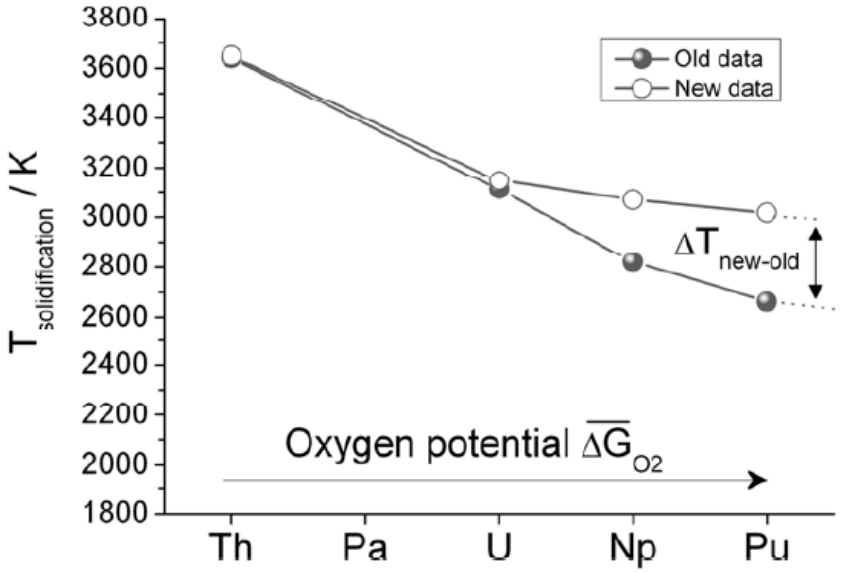

[Manara et al, Procedia Chem. 7 (2012) 505]

The reactivity between actinide oxides (ThO_2, UO_2 , NpO_2, PuO_2) and metallic crucibles (W…)
↗ with the oxygen potential of the actinide oxides

$\mu(O_2)$ in PuO_2 >> $\mu(O_2)$ in UO_2 ➡ PuO_2 loses oxygen at high temperature
➡ The reactivity PuO_2/W is >> than for UO_2/W
➡The melting point for PuO_2 was underestimated due to a reaction with the crucible
➡ **Laser heating with self-crucible is a suitable method**

➡Model for $(U,Pu)O_{2\pm x}$

- Mixed uranium and plutonium dioxide $(U,Pu)O_{2\pm x}$ has a large oxygen composition range

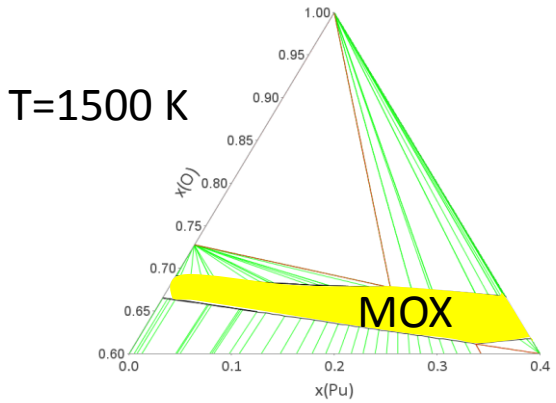

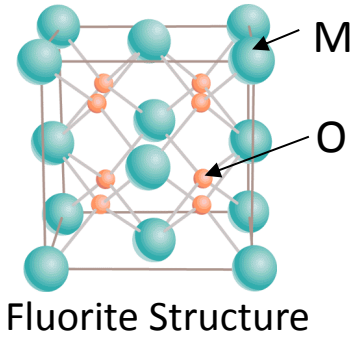

- **Three sublattice model $(U^{+3},U^{+4},U^{+5},Pu^{+3},Pu^{+4})\ (O^{-2},Va)_2\ (O^{-2},Va)$**

  ⇨ Ternary interaction parameters between cations have been adjusted to fit experimental data

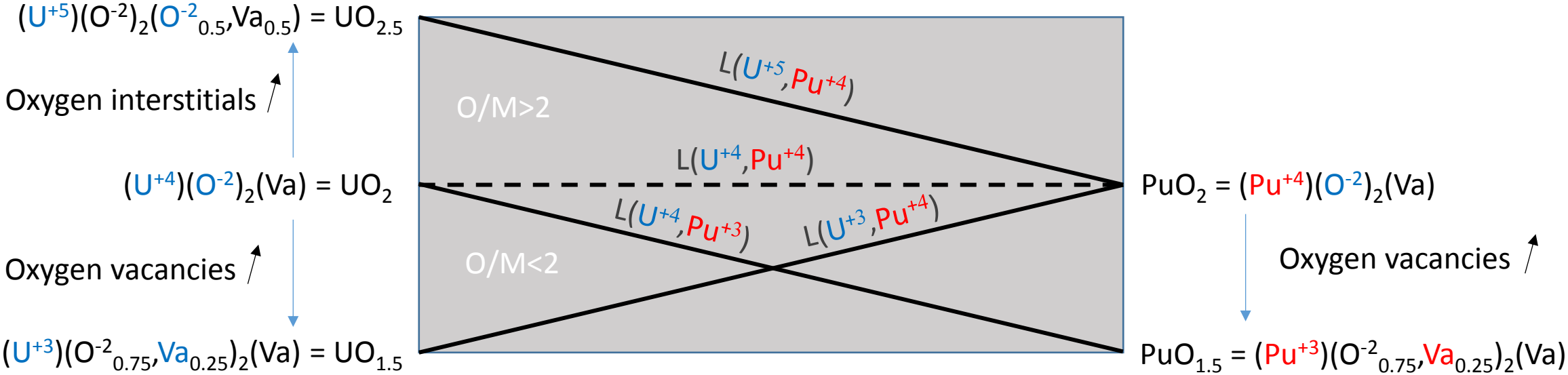

➡ Experimental thermodynamic data for $(U,Pu)O_{2\pm x}$

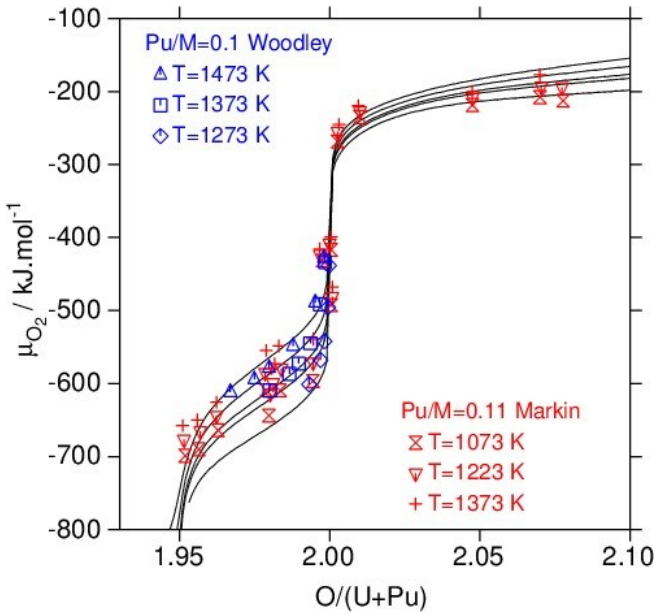

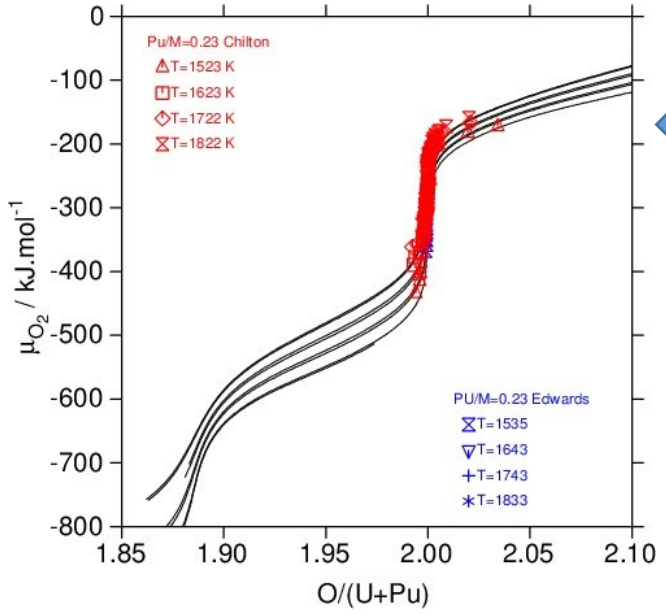

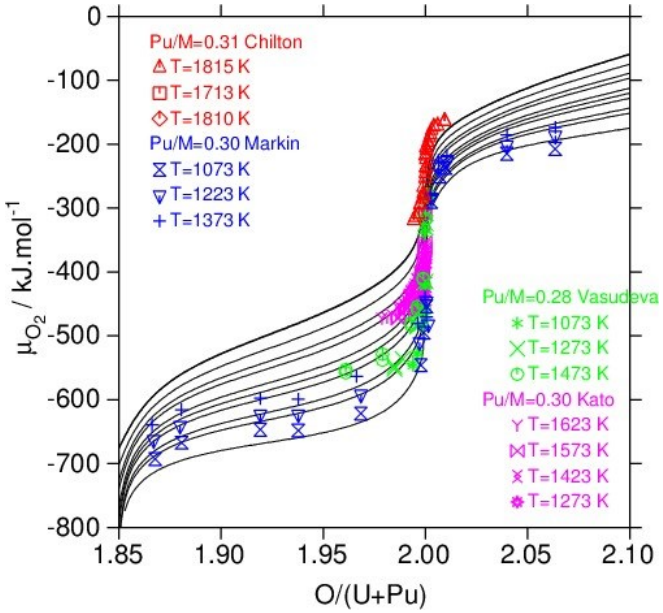

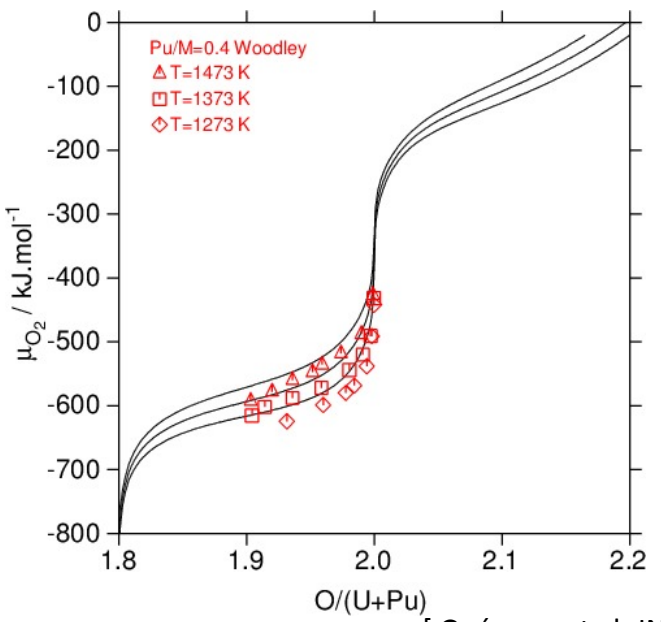

- Oxygen chemical potential data are available for 0.1<Pu/(U+Pu)<0.4

$$\mu_{O_2} = \Delta G(O_2) = R\,T \ln p_{O_2}$$

⇨ **The oxygen potential increases with the Pu content**

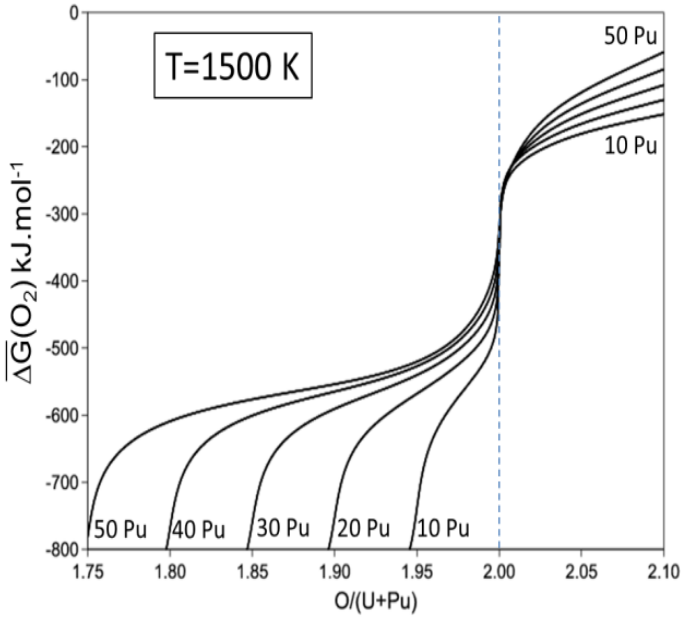

[Guéneau et al, JNM 419 (2011) 145]

➡Defect chemistry in $(U,Pu)O_{2\pm x}$

T=1500 K

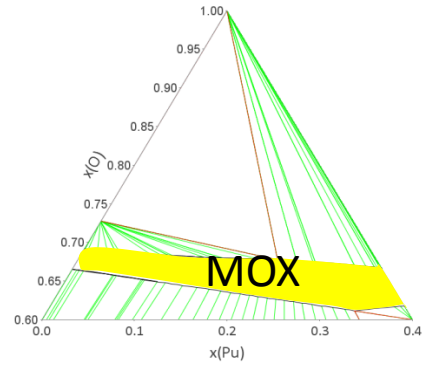

■ **Three sublattice model $(U^{+3},U^{+4},U^{+5},Pu^{+3},Pu^{+4})\ (O^{-2},Va)_2\ (O^{-2},Va)$**

- For O/M<1.9: Oxygen vacancies and $U^{+4} \Rightarrow U^{+3}$, Pu^{+3} — Reduction of U^{+4}
- For 1.9<O/M<2: Oxygen vacancies and $Pu^{+4} \Rightarrow Pu^{+3}$, U^{+4} — Reduction of Pu^{+4}
- For O/M>2: Oxygen interstitials and $U^{+4} \Rightarrow U^{+5}$ — Oxidation of U^{+4}

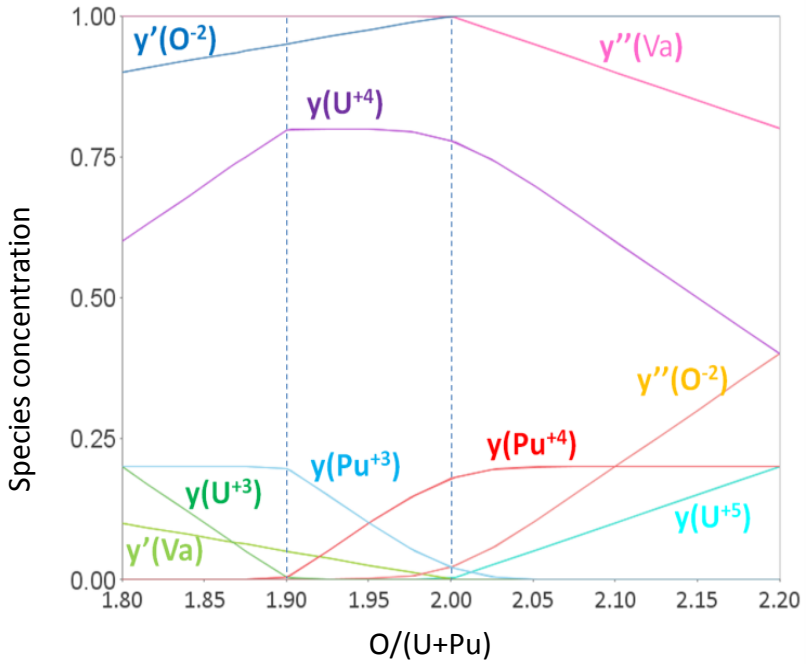

T=1500 K

MOX with 20%Pu

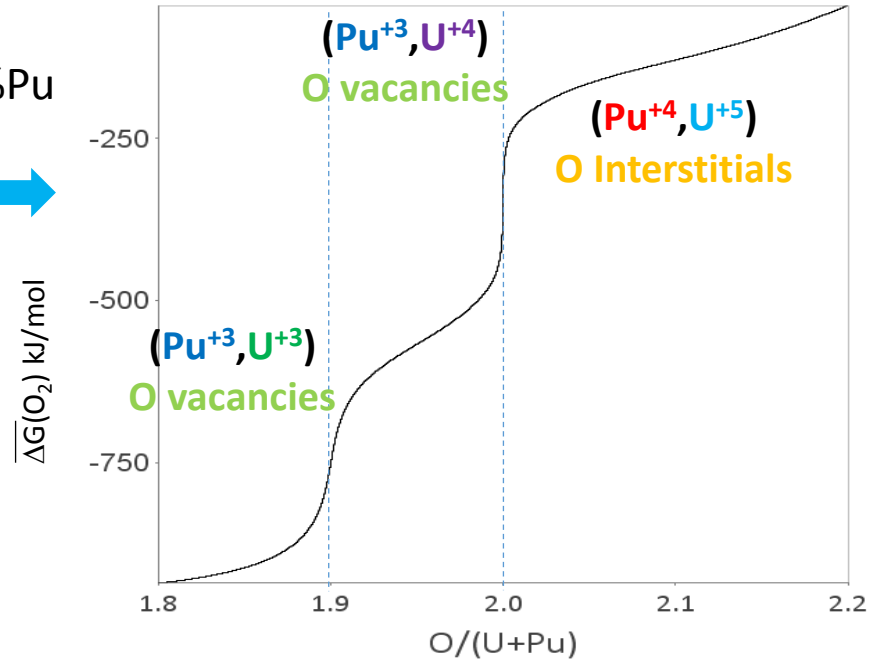

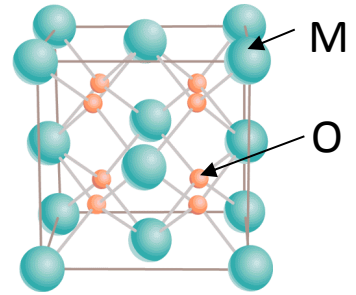

Fluorite Structure

[Guéneau et al, JNM 419 (2011) 145]

➡ UO_2-PuO_2 system

Phase diagram data

Guéneau et al, JNM 2011

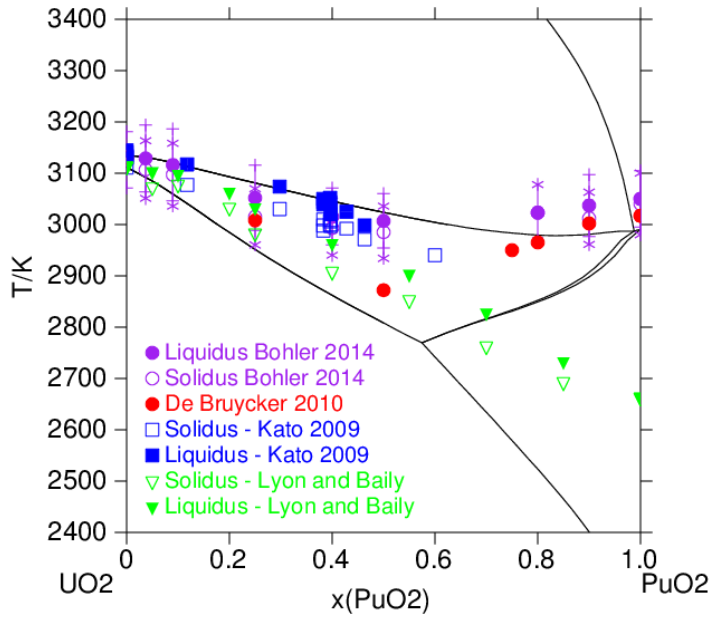

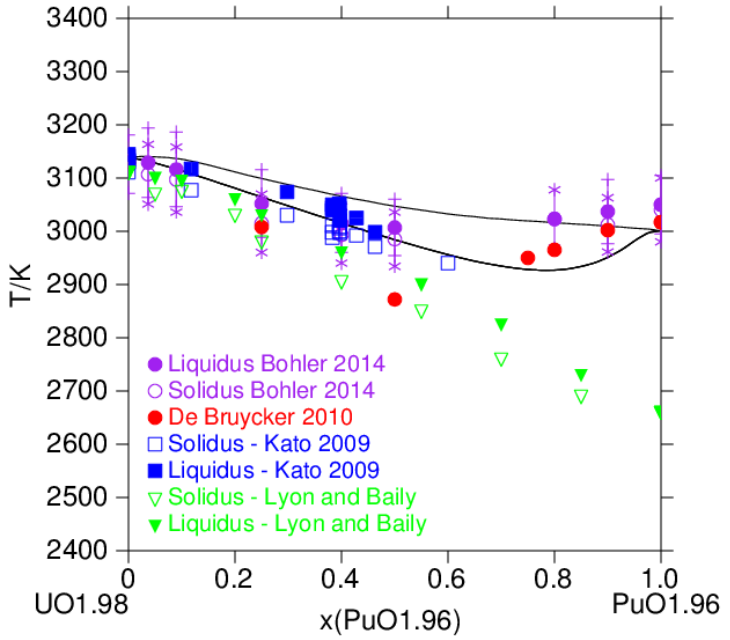

-Lyon and Bailey	➡ « **Reference** » data measured by thermal analysis in **W crucible**
- Kato et al	➡ Thermal analysis with **Re crucible** ➡ Higher solidus / liquidus T
- De Bruycker et al	➡ **Laser heating** ➡ **Consistent with the new melting point of PuO_2 (3017 K).** ➡ **A minimum is found in the liquidus curve**

⇨ The data of Bohler (2014) have to be taken into account to improve the model for the liquid/solid transition

➡Isothermal sections of the U-Pu-O system

At low T: miscibility gap in $(U,Pu)O_{2-x}$

T=473 K

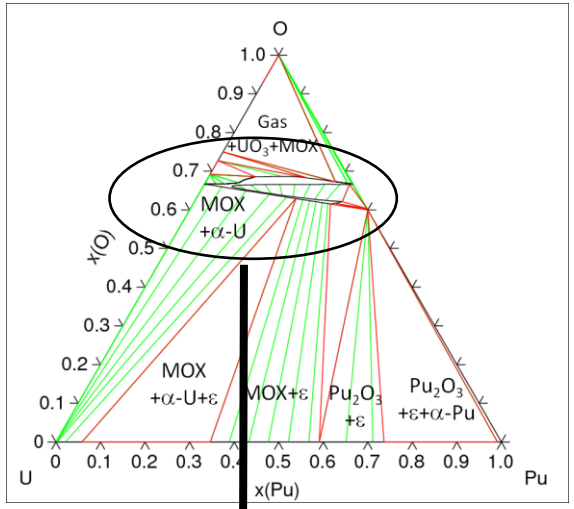

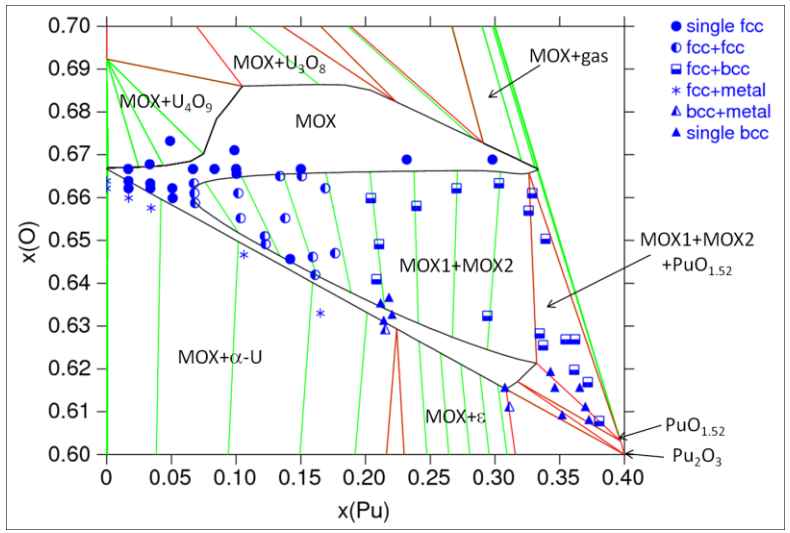

At high T: continuous solid solution $(U,Pu)O_{2\pm x}$

T=1600 K

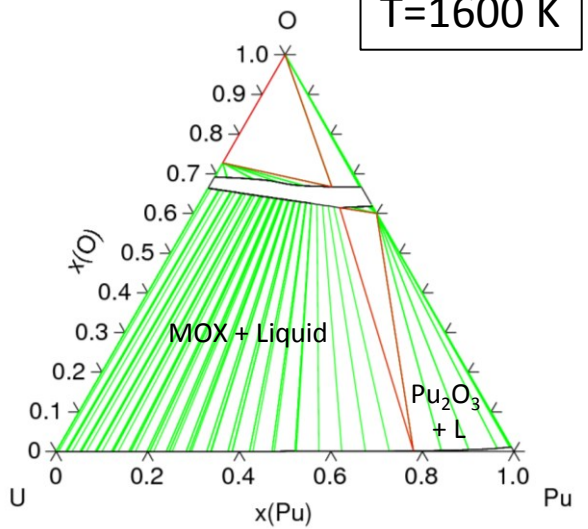

T=2500 K

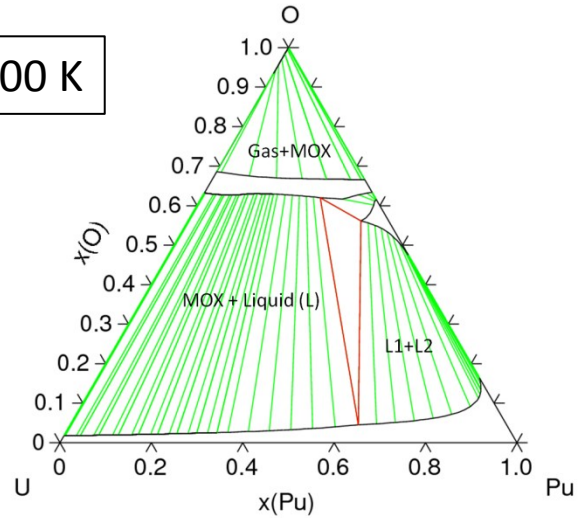

T=3000 K

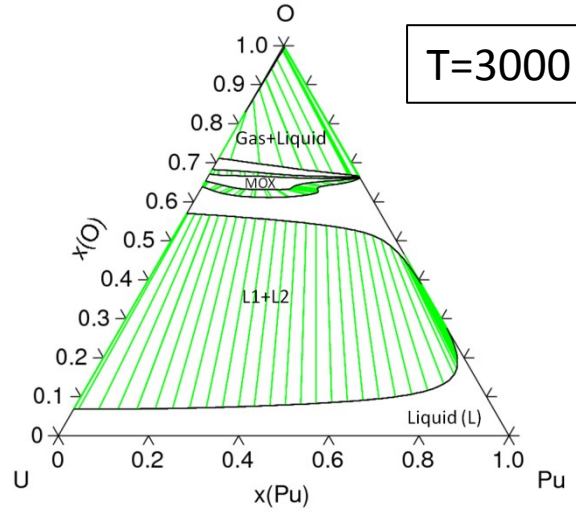

[Guéneau et al, JNM 419 (2011) 145]

➡Thermodynamic parameters for $(U,Pu)O_{2\pm x}$

$(Pu^{+3},Pu^{+4},U^{+3},U^{+4},U^{+5})(O^{-2},Va)_2(O^{-2},Va)$

MOX : $(Pu^{+3},Pu^{+4},U^{+3},U^{+4},U^{+5})(O^{-2},Va)_2(O^{-2},Va)$

$$G^{MOX}_{(U^{+3})(O^{-2})(Va)} = G^{MOX}_{UO_2} - G^{MOX}_{(U^{+4})(Va)(Va)} + G^{MOX}_{(U^{+3})(Va)(Va)}$$

$$G^{MOX}_{(U^{+4})(O^{-2})(Va)} - H^{SER}_{U} - 2H^{SER}_{O} = G^{MOX}_{UO_2} - H^{SER}_{U} - 2H^{SER}_{O}$$
$$= -1118940.2 + 554.00559T - 93.268T\ln T + 1.01704254.10^{-2}T^2$$
$$- 2.03335671.10^{-6}T^3 + 1091073.7T^{-1}$$

$$G^{MOX}_{(U^{+5})(O^{-2})(Va)} = G^{MOX}_{UO_2} - 58351.62 + 39.67611T + 0.69315RT$$

$$G^{MOX}_{(U^{+3})(Va)(Va)} = G^{MOX}_{UO_2} - 2G^{gas}_{O} + 747127 - 70.22618T + 1.12467RT$$

$$G^{MOX}_{(U^{+4})(Va)(Va)} = G^{MOX}_{UO_2} - 2G^{gas}_{O} + 545210.5$$

$$G^{MOX}_{(U^{+5})(Va)(Va)} = G^{MOX}_{(U^{+5})(O^{-2})(Va)} - 2G^{gas}_{O} + 700000$$

$$G^{MOX}_{(U^{+3})(O^{-2})(O^{-2})} = G^{MOX}_{(U^{+3})(O^{-2})(Va)} + G^{gas}_{O}$$

$$G^{MOX}_{(U^{+4})(O^{-2})(O^{-2})} = G^{MOX}_{UO_2} + G^{gas}_{O}$$

$$G^{MOX}_{(U^{+5})(O^{-2})(O^{-2})} = G^{MOX}_{(U^{+5})(O^{-2})(Va)} + G^{gas}_{O}$$

$$G^{MOX}_{(U^{+3})(Va)(O^{-2})} - H^{SER}_{U} - H^{SER}_{O} = G^{MOX}_{(U^{+4})(Va)(O^{-2})} - H^{SER}_{U} - H^{SER}_{O}$$
$$= G^{MOX}_{(U^{+5})(Va)(O^{-2})} - H^{SER}_{U} - H^{SER}_{O} = +100000$$

$$L^{MOX}_{(U^{+4},U^{+5})(O^{-2})(O^{-2})} = -124936.9 - 21.6838T$$

$$L^{MOX}_{(U^{+3},U^{+4})(O^{-2})(Va)} = +40133.7 + 1076.4\left(y_{U^{+3}} - y_{U^{+4}}\right)$$

U-O

Pu-O

$$G^{MOX}_{(Pu^{+4})(O^{-2})(Va)} - H^{SER}_{Pu} - 2H^{SER}_{O} = G^{MOX}_{PuO_2} - H^{SER}_{Pu} - 2H^{SER}_{O}$$
$$= -1099562.8 + 505.428856T - 83.31922T\ln T$$
$$- 0.00584178T^2 - 2.29241167.10^{-11}T^3 + 913506T^{-1}$$

$$G^{MOX}_{(Pu^{+4})(Va)(Va)} = G^{MOX}_{PuO_2} - 2G^{gas}_{O}$$

$$G^{MOX}_{(Pu^{+4})(O^{-2})(O^{-2})} = G^{MOX}_{PuO_2} + G^{gas}_{O} + 80T$$

$$G^{MOX}_{(Pu^{+4})(Va)(O^{-2})} = G^{MOX}_{PuO_2} - G^{gas}_{O} + 80T$$

$$G^{MOX}_{(Pu^{+3})(O^{-2})(Va)} = G^{MOX}_{(Pu^{+3})(Va)(Va)} + 2G^{gas}_{O}$$

$$G^{MOX}_{(Pu^{+3})(Va)(Va)} = 0.5G^{Pu_2O_3} - 1.5G^{gas}_{O} + 3817.7 + 1.12467RT$$

$$G^{MOX}_{(Pu^{+3})(O^{-2})(O^{-2})} = G^{MOX}_{(Pu^{+3})(Va)(Va)} + 3G^{gas}_{O} + 80T$$

$$G^{MOX}_{(Pu^{+3})(Va)(O^{-2})} = G^{MOX}_{(Pu^{+3})(Va)(Va)} + G^{gas}_{O} + 80T$$

$$L^{MOX}_{(Pu^{+3},Pu^{+4})(O^{-2})(Va)} = L^{MOX}_{(Pu^{+3},Pu^{+4})(Va)(Va)} = +9781.9 + 3.06205T$$
$$+\left(y_{Pu^{+3}} - y_{Pu^{+4}}\right)\left(-17507.47 + 5.46573T\right)$$

$$L^{MOX}_{(U^{+4},Pu^{+4})(O^{-2})(Va)} = -20000$$

$$L^{MOX}_{(U^{+4},Pu^{+3})(O^{-2})(Va)} = -150000$$

$$L^{MOX}_{(U^{+3},Pu^{+4})(O^{-2})(Va)} = +20000$$

$$L^{MOX}_{(U^{+4},Pu^{+3})(Va)(Va)} = -300000$$

$$L^{MOX}_{(Pu^{+4},U^{+5})(O^{-2})(*)} = -80000$$

U-Pu-O

[Guéneau et al, JNM 419 (2011) 145]

TAF-ID DATABASE PROJECT (2013-2017)

OECD BETTER POLICIES FOR BETTER LIVES — Nuclear Energy Agency — NEA NUCLEAR ENERGY AGENCY

www.oecd-nea.org/science/taf-id/

(Canada, France, Japan, The Netherlands, Korea, UK, USA)

41 Elements

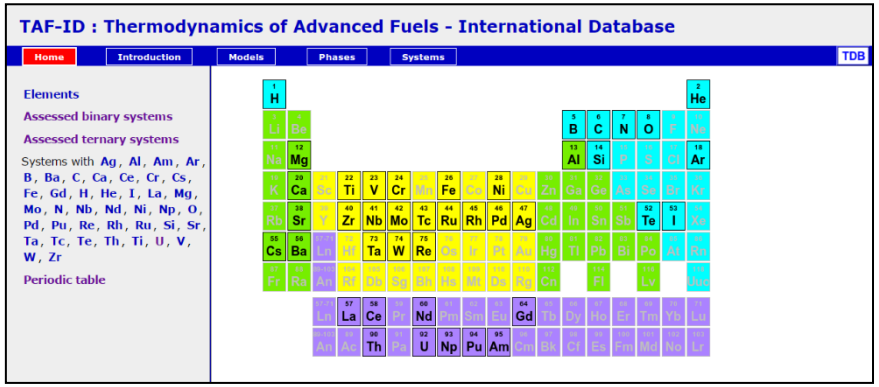

206 Binaries

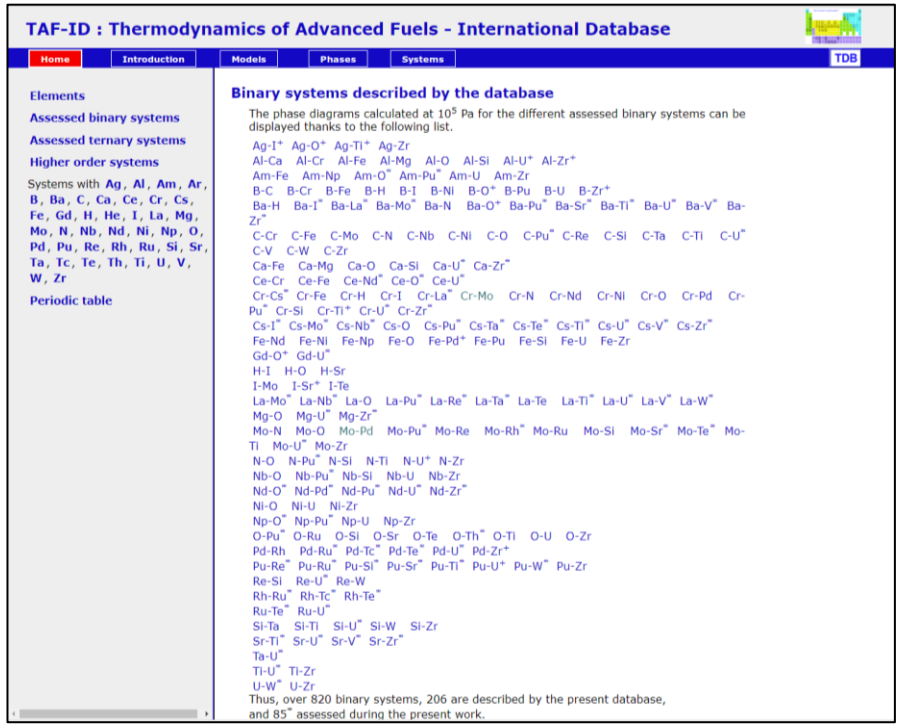

76 Ternaries

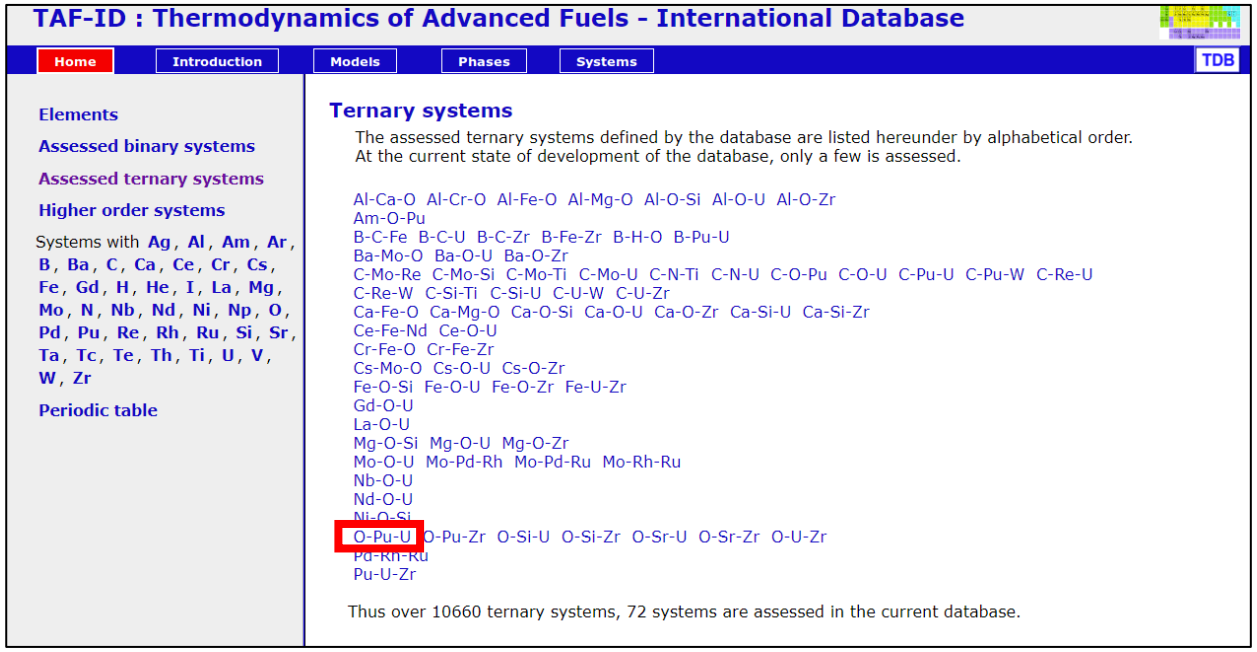

⇨ Phase 2 : Dec. 2019 – Dec. 2022

➡Calculations on irradiated MOX fuel

PREDICTION OF OXYGEN POTENTIAL

Calculation for a MOX fuel with burnups of 3.8, 7 and 11.2 at .%

⇨ 16 Fission Products (Nd,La,Gd,He,Ce,I,Zr,Cs,Sr,Ba,Te,Mo,Pd,Ru,Tc,Rh)

$(U^{+3},U^{+4},U^{+5},Pu^{+3},Pu^{+4},Zr^{+2},Zr^{+4},Ce^{+3},Ce^{+4},Gd^{+3},La^{+3},Nd^{+3})(O^{-2},Va)_2(O^{-2},Va)$

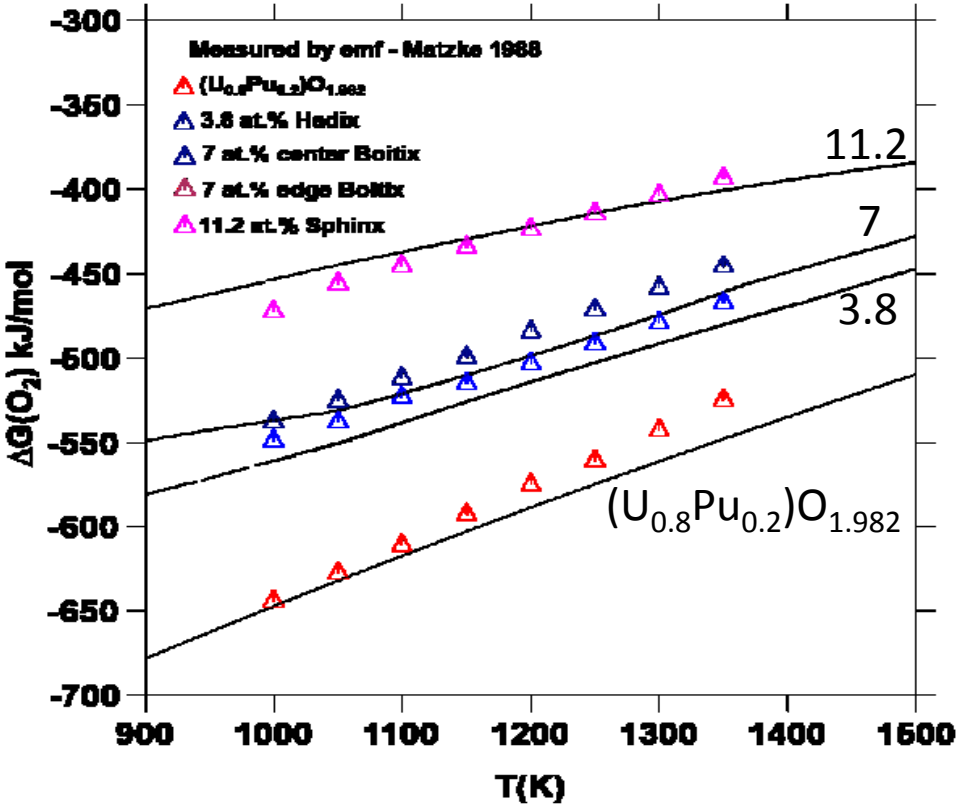

O/M of the oxide matrix at 1600 K

Burnup ↗

1.997
1.996
1.995

O/M ↗

⇨ The oxygen potential of the fuel increases with burnup

⇨ Very good agreement between calc./exp. oxygen potential data

➡Calculations on irradiated MOX fuel

FORMATION OF SECONDARY FISSION PRODUCT PHASES FOR A 7 at. % BURNUP

1500 < T(K) < 3500

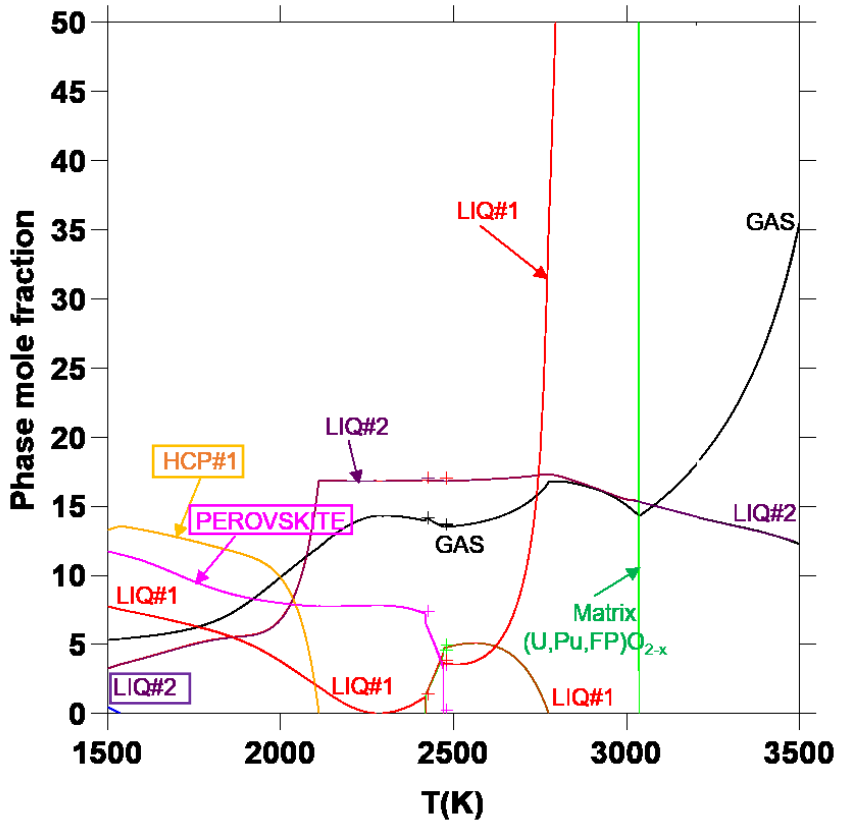

Matrix $(U,Pu,FPs)O_2$ matrix
+ Metallic precipitates (HCP)
+ Perovskite precipitates
+ Liquid phases
+ Gas

➡ Typical microstructure of a MOX fuel pellet irradiated at 13% in a Fast reactor (PHENIX)

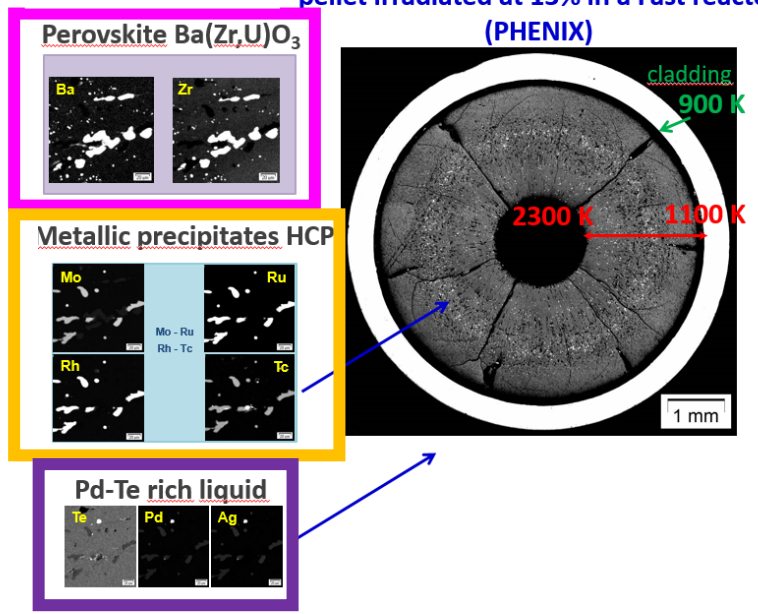

Metallic precipitates (HCP)
Melting
at T=2109 K

Perovskite $(Ba,Sr)(Zr,U)O_3$
Melting
at T=2469 K

➡ Dissolution of the fuel matrix in the molten perovskite ➡ Beginning of the oxide fuel melting

➡ Conclusion

- Thermodynamic modelling of nuclear fuels is required to provide key input thermodynamic and phase diagram data for Fuel Performance Codes
  - ⇨ Oxygen potential, fission product phases (JOG/ROG formation), solid/liquid transitions, heat capacity ….

- CALPHAD is a suitable method to model multi-component systems by extrapolating from binary and ternary sub-systems;
  - ⇨ It is time consuming ⇨ International collaborative projects are good frameworks to develop large databases
  - ⇨ Experimental thermodynamic measurements on fuels are challenging but needed to test the validity of the databases (Phase 2 of TAF-ID project)
  - ⇨ First-principle calculations are useful to calculate thermodynamic data that can be used in the models

- But thermodynamics (alone) cannnot explain the fuel behaviour; it has to be coupled with kinetic and mass transfer models
  - ⇨ In the GERMINAL fuel performance code, there is a coupling using the open source code Open Calphad (developped by Bo Sundman) and the TAF-ID database

- Other Gibbs energy minimizer codes exist such as FACTSAGE, PANDAT, PyCALPHAD …
  - ⇨ The format of the database can differ; in some cases a conversion of the database file is required (for instance from Thermo-Calc to FACTSAGE format);
  - ⇨ All the sublattice models are not implemeted in all the codes

TAF-ID website: https://www.oecd-nea.org/science/taf-id/
A public version is available ⇨ contact person: davide.costa@oecd.org